A Review of Experimental Methods for Characterizing Ferroelectric Domain Dynamics in Relaxor-$PbTiO_3$ Single Crystals

Jeong-Woo Sun, Zhengze Xu, Sang-Goo Lee, Wook Jo, Xiaoning Jiang, *Fellow, IEEE*, and Jong Eun Ryu

***Abstract*—Relaxor-based ferroelectric single crystals possess colossal piezoelectric and dielectric properties and have been attractive for a wide range of electromechanical applications including transducers, sensors, and actuators. However, domain dynamics of relaxor ferroelectric single crystals are still not fully understood despite significant progress in the last three decades, partly because of the combined relaxor and normal ferroelectrics with complex domain structures within the material. Without a comprehensive understanding of domain dynamics, rational domain engineering for high piezoelectricity is challenging. In this review, we review experimental methods for characterizing domain dynamics in nanoscale and bulk mesoscale that exhibit both intrinsic and extrinsic contributions. We focus on literature published since 2010 and critically evaluate their strengths and limitations. From an overview of recent understanding, we highlight the need for real-time observations at appropriate time and length scales and cross-validation of different methods for precise measurements of domain dynamics.**

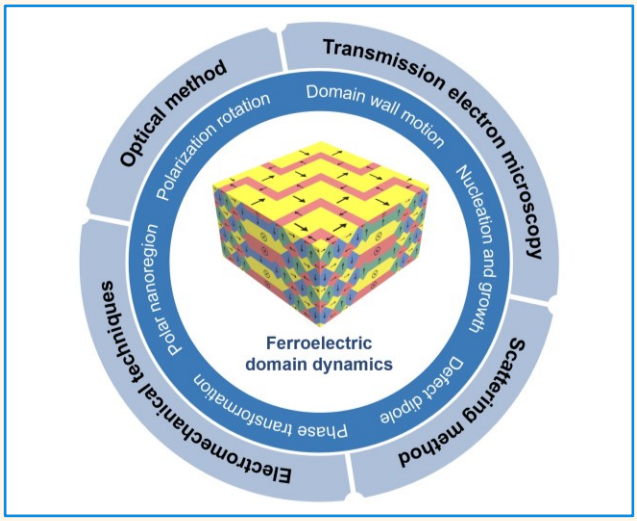

***Index Terms*—Ferroelectrics, Piezoelectrics, Domain engineering, Polarization rotation, Domain wall motion, Relaxor-PT single crystals**

I. Introduction

Ferroelectricity is characterized by spontaneous polarization which can be switchable by an external electric field. Ferroelectric materials exhibit diverse properties, including pyroelectricity and non-linear dielectric behavior, which have led to their application in various technologies. These applications include ferroelectric memory devices [1, 2], pyroelectric sensors [3], energy storage systems [4, 5], and flexible electronics [6]. Notably, ferroelectrics can also possess piezoelectricity, allowing them to accumulate electrical charge upon mechanical stress or vice versa. In their virgin state, ferroelectric domains are disordered, which diminishes piezoelectric effects due to the differing orientations of these domains. However, when an electric field above the coercive field (E_C) is applied, ferroelectrics can achieve an aligned domain configuration and retain remanent polarization (P_r) even after the field is removed. This process, known as electrical poling, is a post-treatment method used to align randomly oriented domains along a specific direction [7]. As a result of this ability to control domain orientation, numerous applications have been developed for electromechanical systems, including actuators [8, 9], sensors [10], nanogenerators [11], electro-optic devices [12], transducers [13, 14], and biomedical devices [15]. Therefore, understanding domain dynamics is crucial in elucidating the correlation between domain engineering and piezoelectricity.

Relaxor-based ferroelectric single crystals have attracted significant attention due to their outstanding piezoelectric

This work was in part supported by NSF under grants # DMR 2011978 and DMR-2309184, and by ONR under Grant # N00014-21-1-2058.

Jeong-Woo Sun is with the Department of Materials Science and Engineering, Ulsan National Institute of Science and Technology, Ulsan 44919, South Korea, and also with the Department of Mechanical and Aerospace Engineering, North Carolina State University, Raleigh, NC 27695 USA (e-mail: jwseon@unist.ac.kr)

Zhengze Xu, Xiaoning Jiang, and Jong Eun Ryu are with the Department of Mechanical and Aerospace Engineering, North Carolina State University, Raleigh, NC 27695 USA (e-mail: zxu43@ncsu.edu; xjiang5@ncsu.edu; jryu@ncsu.edu)

Sang-Goo Lee is with iBULe Photonics Inc., Incheon 21999, South Korea (e-mail: sanggoo7@ibule.com)

Wook Jo is with the Department of Materials Science and Engineering, Ulsan National Institute of Science and Technology, Ulsan 44919, South Korea (e-mail: wookjo@unist.ac.kr)

Highlights

- **In relaxor-based ferroelectric single crystals, domain dynamics are complex yet crucial for various piezoelectric applications such as transducers and sensors.**
- **Despite substantial progress, understanding of domain dynamics remains incomplete due to the intricate structure of materials, which hinders rational domain engineering.**
- **This review evaluates experimental methods for characterizing domain dynamics and highlights the necessity of real-time observations and cross-validation of different analyses.**

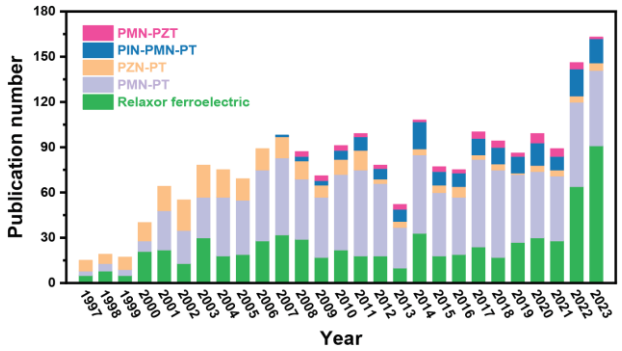

Fig. 1. Publications of different relaxor ferroelectric single crystals since 1997. Search on Web of Science for "Single crystal" and "Relaxor ferroelectric", "PMN-PT", "PZN-PT", "PIN-PMN-PT", or "PMN-PZT" in the topic, title, or abstract.

coefficient (d_{33} > 1500 pC/N) and electromechanical coupling factor (k_{33} > 0.90) [16-18]. The first generation of relaxor-$PbTiO_3$ (relaxor-PT) single crystals consisted of binary systems such as $Pb(Mg_{1/3}Nb_{2/3})O_3$-$PbTiO_3$ (PMN-PT) or $Pb(Zn_{1/3}Nb_{2/3})O_3$-$PbTiO_3$ (PZN-PT). Since 2007, second and third generations of ternary or doped systems have been developed, including $Pb(In_{1/2}Nb_{1/2})O_3$-$Pb(Mg_{1/3}Nb_{2/3})O_3$-$PbTiO_3$ (PIN-PMN-PT) and $Pb(Mg_{1/3}Nb_{2/3})O_3$-$PbZrO_3$-$PbTiO_3$ (PMN-PZT), to further enhance functionality (See Fig. 1).

Numerous studies have investigated the origin of high piezoelectricity in relaxor-PT single crystals. Key findings suggest that the monoclinic phase may enhance piezoelectricity due to its multiple polarization directions [19-24]. Additionally, polarization rotation can increase piezoelectric responses, with larger rotation angles leading to greater effects [25-30]. Electric field-induced phase transformation has also been linked to the exceptional strain and piezoelectric coefficient observed in these materials [16, 31-35]. Furthermore, polar nanoregions (PNRs) within relaxor-PT systems may influence piezoelectric behaviors due to their local structural heterogeneity and flat energy landscape, which features low activation energy for polarization switching [36-40]. Despite extensive research into the mechanisms underlying the ultrahigh piezoelectric properties of relaxor-PT crystals, debate persists regarding poling-dependent characteristics, particularly the effects of direct current (DC) poling and alternating current (AC) poling. Some studies suggest that reducing domain size and increasing domain wall density can improve piezoelectricity [41-47], whereas others propose that enlarging domain size contributes to the effectiveness of AC poling [48-53]. Given that ferroelectric domain characteristics significantly influence piezoelectricity, continued study of domain dynamics is essential for understanding the performance of relaxor ferroelectric single crystals.

Traditional experimental methods for analyzing domain dynamics include piezoelectric force microscopy (PFM) [54-56], polarized light microscopy (PLM) [57, 58], and X-ray diffraction (XRD) [59, 60]. These techniques are typically complemented by charge-coupled devices (CCDs) with high frame rates and *in-situ* measuring equipment for pressure, electric field, or temperature to facilitate the investigation of domain dynamics. However, PFM examines surface features within a restricted area, potentially failing to represent the bulk structure in ferroelectric materials which exhibit depth dependence on the order of micrometers [61-64]. While PLM offers a large spatial depth of several hundred microns, it is limited to identifying ferroelectric domains with distinct optical properties, and domain overlap along the observation direction can hinder accurate structural analysis [65, 66]. Although XRD effectively evaluates bulk response, it has limitations in refinement selection regarding inhomogeneous domain size [67-69]. Therefore, comprehensive analysis of ferroelectric domains requires multiple methods or advanced measurement techniques to ensure consistency between structural and macroscopic behavior.

This review provides a comprehensive overview of characterization methods for relaxor ferroelectric single crystals, with particular emphasis on domain dynamics including polarization rotation, domain wall motion, phase transformation, and their effect on piezoelectricity. The paper has three primary objectives: First, we establish correlations between ferroelectric domain dynamics and piezoelectric properties. Because ferroelectric domain characteristics determine piezoelectricity, understanding domain dynamics is crucial for explaining the properties of relaxor-PT crystals. Second, we identify the mechanisms that govern ferroelectric domains. Understanding the driving forces and complex processes of domain dynamics is necessary to optimize material performance. Third, we examine the relationship between domain dynamics and ferroelectric phases, such as monoclinic phases and polar nanoregions (PNRs).

II. Optical Method

Given the phase instability of relaxor-PT single crystals [36, 70, 71] and their susceptibility to structural and electrical changes [72, 73], noncontact and nondestructive optical methods have been developed to investigate domain dynamics. PLM exploits optical anisotropy to study domain formation in

TABLE I
EXPERIMENTAL METHODS FOR CHARACTERIZING FERROELECTRIC DOMAIN DYNAMICS

Experimental method	Technique	Capability in Domain Dynamics	Advantage	Inadequacy or Limitation
Optical method	Polarized light microscopy (PLM) [57], Birefringence imaging microscopy (BIM) [86], Quantitative PLM [53], Second harmonic generation (SHG) [102], Raman spectroscopy [116]	- Birefringence and optical anisotropy from different orientation of polarization - Domain dynamics with noncentrosymmetric properties	- Nondestructive and noncontact evaluation - Quantification of ferroelectric domain walls - Determining the symmetry of domain walls	- Challenging to extract local information of mixed phases and monoclinic structure simultaneously
Transmission electron microscopy	*In-situ* transmission electron microscopy (TEM) [128, 131], Scanning transmission electron microscopy (STEM) [22]	- Investigating domain structure and dynamics at atomic and subatomic levels - Distinct contrast of ferroelectric domains with spatial resolution reaching up to ~1 nm	- High-resolution imaging and polarization vector of individual unit cells - Detecting dispersed polar states with multiphase structures	- Destructive for sample preparation - Electron beam-induced irradiation damage, charging effect, or polarization switching
Scattering method	X-ray diffraction (XRD) [161, 163], Neutron scattering [38], X-ray photon correlation spectroscopy (XPCS) [194]	- Determining crystal structure-property relation - Diffuse scattering about the dynamics of short-range correlated atomic displacements	- Effective for evaluating the bulk domain structure - Time-resolved investigation of structural evolution or domain dynamics	- Requirement of high energies and beamline facilities as needed - Difficult accessibility of neutron sources
Electro-mechanical technique	Piezoresponse force microscopy (PFM) [202, 212], Vertical PFM (v-PFM), Lateral PFM (l-PFM)	- Inverse piezoelectric effect via a conductive tip - Visualization of domain morphology by amplitude and phase	- Three-dimensional surface maps with vertical and lateral directions - Imaging and domain dynamics in a liquid environment	- Surface features may differ from bulk structures, not representing macroscopic properties - Skin effect due to the low penetration depth (< 10 nm)

various orientations relative to spontaneous polarization, and *in-situ* PLM enables studies of high-temperature poling and domain wall motion [74-81]. For example, domain configurations in pure rhombohedral PMN-22PT [78] and pure tetragonal PMN-60PT [74] exhibit extinction angles (θ) at $\theta = 45°$, and $\theta = 0°$ or 90°, respectively, due to the distinct contrast between rhombohedral and tetragonal phases under PLM observation. However, relaxor ferroelectric single crystals near the morphotropic phase boundary (MPB) often contain mixed phases or monoclinic structures, resulting in complex PLM images of micro-/nanoscale domain structures [82, 83]. Although the observed irreversible domain switching may induce phase coexistence and enhance piezoelectricity through large polarization rotation [57, 75], extracting local information about domain walls and phase differences from PLM results remains challenging. To address these limitations, Birefringence imaging microscopy (BIM) employs a rotating polarizer and circular analyzer to observe the full-angle rotation [84]. BIM provides detailed information about domain structures and their spatial distribution. Several BIM studies have characterized domain walls in alternating current (AC) poled rhombohedral PMN-PT crystals with ultrahigh transparency [48, 85]. Luo *et al.* investigated domain walls and phase transformations in $BiScO_3$-$PbTiO_3$ (BS-PT) single crystals near the MPB (Fig. 2) [86]. Their observations showed that domain walls gradually disappeared as temperature increased up to 500 °C, accompanied by fluctuations in both the angle φ and phase shift $|\sin \delta|$ at lower temperatures. The system underwent a transformation from a multi-domain state to a homogeneous tetragonal state at 385 °C, followed by a tetragonal-to-cubic transformation at 460 °C. Although BIM effectively reveals both domain walls and phase transformations, it has limitations in distinguishing between mixed phases or identifying monoclinic phases.

To facilitate quantitative assessment of birefringent materials, quantitative PLM (QPLM) has been developed [87-89]. The apparent birefringence (Δn) is given by

$$\Delta n = \frac{\phi \lambda}{2\pi t}, \tag{1}$$

where ϕ is the retardation, λ is the wavelength of the light source, and t is the sample thickness. Although the

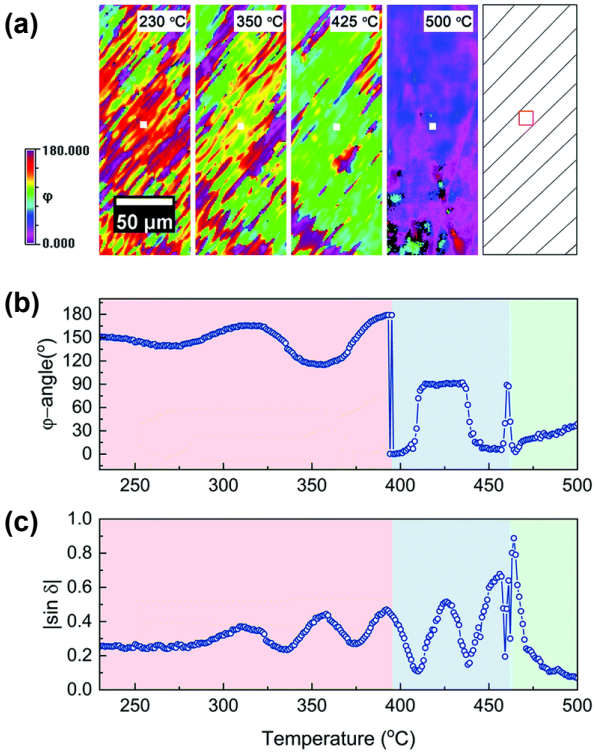

Fig. 2. (a) Measured birefringence imaging microscopy (BIM) images of the orientation distributions at 230 °C, 350 °C, 425 °C, and 500 °C and the schematic presentations of the domain structures of a [100]-oriented 0.324BS-0.676PT single crystal. (b) The temperature dependence of the average orientations and (c) $|\sin \delta|$ of selected areas. The data reproduced with permission from [86].

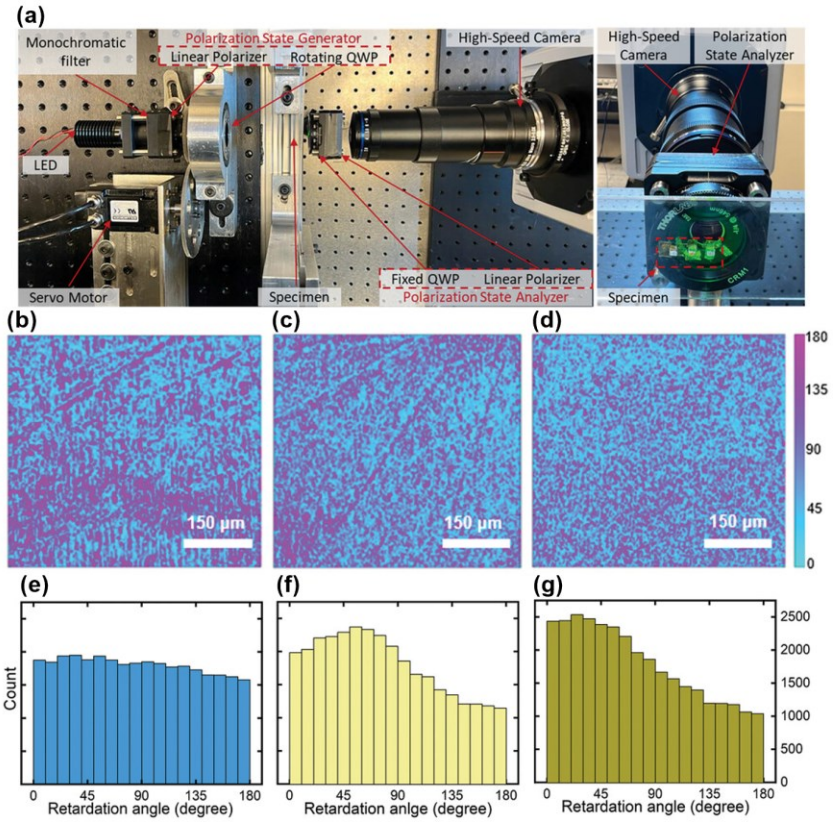

Fig. 3. (a) Experimental setup of the QPLM measurement. (b)-(d) Retardation maps (in degrees) obtained for unpoled (b), low-cycle alternating current (AC) poled (c), and high-cycle AC poled (d) rhombohedral PMN-PT single crystals. (e)-(g) The corresponding histograms for the retardation maps are also shown for unpoled (e), low-cycle AC poled (f), high-cycle AC poled (g) crystals. The retardation maps and histograms were obtained for five locations on the samples and the average alignment degree (φ) value is used to calculate the apparent birefringence for each sample. The data reproduced with permission from [53].

birefringence from QPLM is not the actual birefringence of ferroelectric materials, changes in birefringence can provide information about domain wall density and orientation that reflect optical anisotropy. Recently, A. Negi *et al.* employed QPLM to observe domain walls and measure domain wall density by comparing low-cycle and high-cycle AC poling of rhombohedral PMN-PT single crystals (Fig. 3) [53]. Unpoled (UP) samples showed random domain wall orientations, whereas AC-poled samples exhibited asymmetric domain walls. The average Δn was calculated to be 0.00069 for UP, 0.00057 for low-cycle AC poling, and 0.00062 for high-cycle AC poling, with lower domain wall density in low-cycle AC poling due to increased domain size. While QPLM is effective for quantifying ferroelectric domain walls of relaxor-PT single crystals, *in-situ* measurements are necessary to investigate domain dynamics under external stimuli such as temperature or electric field.

Second harmonic generation (SHG) is a nonlinear optical process sensitive to point symmetry violations in ferroelectrics, such as crystal structures and engineered domains [90-98]. Relaxor ferroelectric single crystals have been investigated using SHG to study domain wall evolution with electric field dependence [99], PT content-dependent nonlinearity [100], and optical properties [101]. Additionally, SHG has been instrumental in detecting monoclinic symmetry, which explains the large piezoelectricity in relaxor-PT single crystals. For example, J. Kaneshiro *et al.* revealed the monoclinic symmetry of PZN-9PT single crystals with MPB composition using SHG microscopy and polarization-dependent maps [102, 103]. However, SHG may yield results inconsistent with theoretical predictions. In $LaAlO_3$ ferroelectric single crystals, a domain wall with *3m* symmetry is unpredictable using other crystallographic methods [104, 105]. It also remains ambiguous how SHG-derived symmetry relates to microstructure. Although the loss of inversion symmetry is established, polarization observations can be uncertain regarding domain wall types and ferroelectric properties. Therefore, SHG analysis should be cross-validated with phase composition and crystal structure to effectively characterize domain walls.

Raman spectroscopy and imaging have been employed to analyze domain dynamics through the inelastic scattering of photons by molecular vibrations [106-112]. These methods elucidate the vibrational modes of crystal structure, which are sensitive to lattice and ferroelectric domains. Raman spectroscopy can identify monoclinic heterophases in relaxor ferroelectric single crystals with large piezoelectric properties [24]. The evolution of Raman peaks as a function of temperature can indicate phase transformations [113, 114]. High-pressure Raman spectroscopy also shows that pressure can suppress local ferroelectric polarization [115]. Similarly, Raman imaging methods can investigate domain dynamics. S. Tsukada *et al.* visualized changes in polarization direction using Raman mapping, where the slowing down of polarization fluctuations and enhanced dielectric response are characterized by smaller ferroelectric domains [116]. In

summary, optical methods are effective for nondestructive and noncontact investigations of domain dynamics, including polarization orientation, noncentrosymmetric properties, and phase transformations of relaxor-PT single crystals. However, there are limitations in simultaneously extracting information about mixed phases and monoclinic structures using a single method.

III. Transmission Electron Microscopy

Transmission electron microscopy (TEM) is an imaging method that employs an electron beam, where the shorter wavelength of electrons enables nanoscale structural information. A widely used technique for imaging ferroelectric domains is scattering contrast, specifically dark-field/bright-field imaging, which provides strong contrast with spatial resolution up to ~1 nm [117-124]. Dark-field images are produced using the selected diffraction beam, whereas bright-field images are generated by selecting only the transmitted beam. Domain configuration can be observed through changes in bright or dark contrast using the scattering contrast mode. Particularly, *in-situ* TEM has been valuable for investigating real-time domain switching phenomena of relaxor ferroelectric single crystals under applied electric field or pressure [125-129]. For example, Y. Sato *et al.* utilized *in-situ* TEM to study domain responses in PMN-30PT single crystals under an external electric field (Fig. 4) [128]. The irreversible redistribution of nanodomains after electric field application could be the origin of remanent polarization and piezoelectricity, suggesting the presence of energetically metastable or stable domain configuration. Their findings indicate that nanoscale domain wall movement contributes to the huge piezoelectric properties of ferroelectric crystals. In related studies, both reversible and irreversible domain switching was observed at various mechanical stress levels in PMN-38PT [130, 131] and 24PIN-PMN-32PT [132] crystals. Fig. 5 demonstrates that at low stress levels (~350 MPa), the tetragonal domains in PMN-38PT exhibit reversible deformation, where the domain structure fully recovers after stress removal due to significant energy barriers created by the pinning effect [133-135]. In contrast, as shown in Fig. 6, when loading exceeds 1250 MPa, PMN-38PT domains undergo irreversible changes. This occurs because the switched

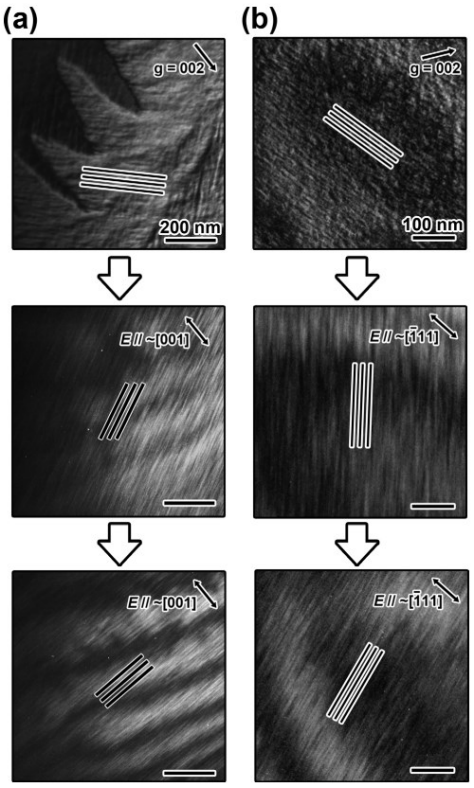

Fig. 4. Two-step redistribution of nanodomains under electric fields. (a) A series of dark-field TEM images without electric field (top), roughly about 20 s (middle) and 40 s (bottom) after start biasing. Electric fields of 10.8 kV/cm are applied parallel to [001]. (b) Another series of dark-field TEM images without electric field, roughly about 30 s and 60 s after start of biasing. Electric fields of 3.3 kV/cm are applied parallel to [111]. Nanoscale domain walls are shown by sets of lines. Scale bars represent 200 nm and 100 nm in (a) and (b), respectively. The data reproduced with permission from [128].

polarization accumulates sufficient energy to overcome nucleation barriers, resulting in altered domain structures upon load release. While *in-situ* TEM results have confirmed the interaction between polarization and electric field or pressure in relaxor-PT single crystals, it is crucial to differentiate between reversible and irreversible properties of external stimuli-induced domain dynamics, as reversible domain switching has also been observed at electric fields above E_C [127, 136]. Furthermore, these interactions may be complicated by applied and built-in electric fields or charging

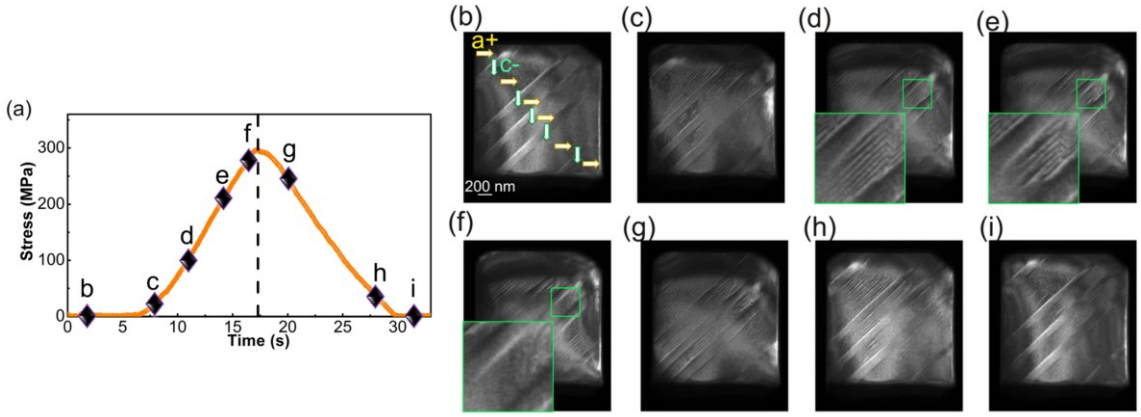

Fig. 5. (a) A load–time curve showing real-time application of tensile loading. Points from b to i correspond to the stress applied to the sample at (b)-(i). (b)–(i) A series of TEM images showing domain evolution at low tensile stress levels. The data reproduced with permission from [131].

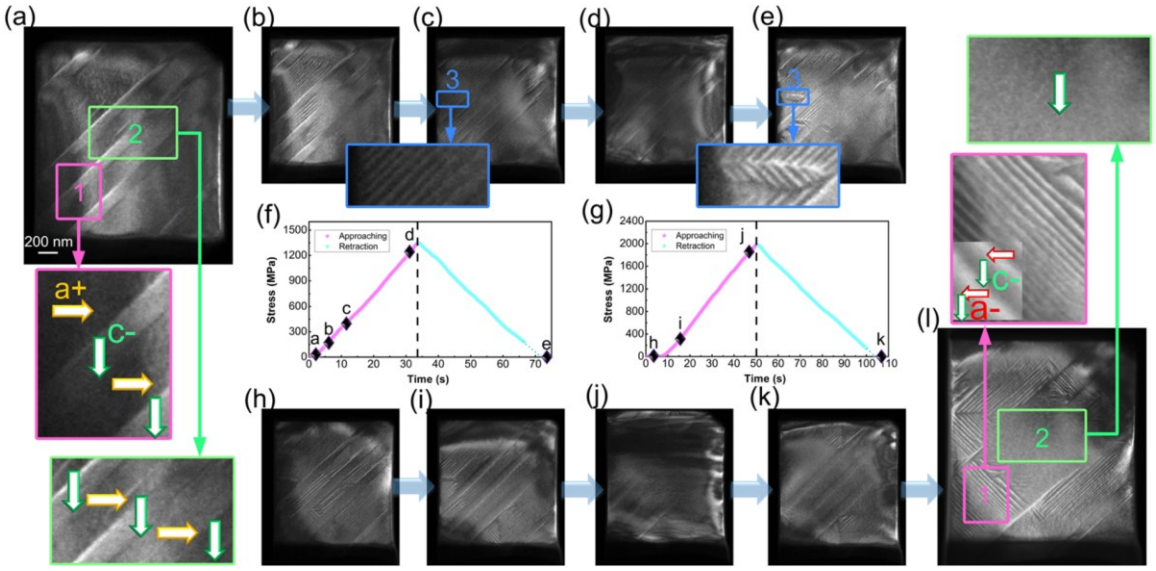

Fig. 6. (a)-(e) A series of TEM images showing domain evolution at medium levels of tensile stress. The corresponding stress-time plot is shown in (f). Labels (a)-(e) in (f) represent the stress applied at the moments shown in (a)-(e). (h)-(l) TEM images showing in-situ deformation of the same pillar as in (a)-(e) at high levels of tensile stress. The corresponding stress-time plot is shown in (g). Labels (h)-(k) in (g) represent the stress applied at the moments shown in (h)-(k). (l) The domain morphology 20 min after domain relaxation in (k). The data reproduced with permission from [131].

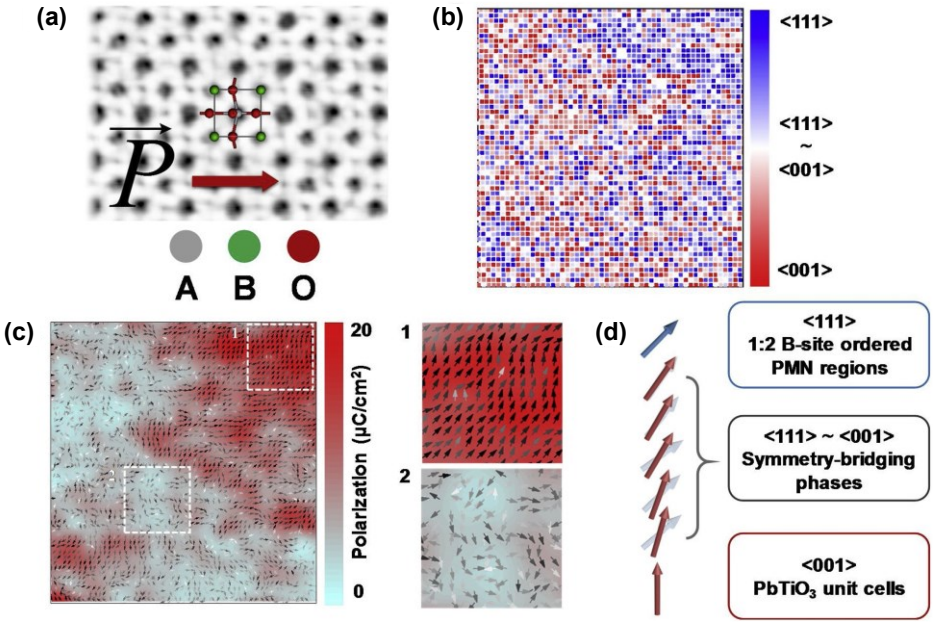

Fig. 7. STEM analyses of the PMN-PT single crystals. (a) A high-angle annular dark-field (HAADF) image of rhombohedral PMN-29PT single crystal. A schematic illustration of the spontaneous polarization in a unit cell is exemplarily given in the inset annular bright field (ABF) image. (b) A map of polarization vectors assigned to crystallographic directions, i.e., tetragonal <001> and rhombohedral <111>. (c) A vector map calculated for each unit cell from atomic column projection. The strength of polarization is expressed as a color map and the color of arrows; darker arrow means stronger and brighter weaker. The arrows indicate the direction of polarization vectors projected on (001) plane. (d) A schematic illustration of polarization types in the polarization map. The data reproduced with permission from [22].

effects during polarization switching, resulting in more complex switching behaviors. Although artifacts such as irradiation damage or electron beam-induced polarization switching can occur during TEM experiments, these effects have not yet been reported in relaxor ferroelectric single crystals.

Scanning transmission electron microscopy (STEM), while similar to TEM in its use of a transmitted electron beam, differs by employing a focused electron beam to scan the material point by point, enabling observation of atomic arrangements and domain dynamics [137-144]. STEM can determine the polarization vector of individual unit cells based on local atomic structures derived from image contrast. The technique is advantageous for detecting dispersed polar states with multiphase structures, including rhombohedral, tetragonal, and monoclinic phases. Numerous studies of relaxor-PT single crystals using STEM have been reported, with their observed heterogeneity helping to explain the outstanding piezoelectric properties of the materials [22, 83, 145-149]. For example, A. Kumar *et al.* investigated polarization, domain dynamics, and heterogeneity distribution in PMN-10PT (low PT content) and PMN-30PT (high PT content) single crystals [146]. Their research revealed a

correlation between the spatial distribution of structural heterogeneities and polarization domain walls. These findings suggest that designing materials with enhanced piezoelectric properties should involve balancing ordered and disordered structure to optimize the distribution of barriers for polarization rotation. As shown in Fig. 7, H.-P. Kim *et al.* employed high-resolution STEM to examine the polarization states of PMN-29PT single crystals at the atomic scale [22]. Their work suggested the presence of a buffer phase that bridges tetragonal and rhombohedral unit cells, with a polarization direction spanning the monoclinic symmetry. The exceptional piezoelectricity of relaxor-PT crystals may arise from synergic interactions between inherently coexisting relaxor ferroelectrics and normal ferroelectrics. In other studies, STEM investigations have revealed the effects of dopants in relaxor-PT single crystals. F. Li *et al.* studied the domain configuration of Sm-doped PMN-PT single crystals [83], finding that Sm dopants enhanced local structural heterogeneity, as indicated by fluctuations in A-sublattice parameters and c/a ratios. The increased heterogeneity correlates with enhanced domain texturing and improved piezoelectric properties. In conclusion, TEM enables investigation of domain structure and kinetics at atomic levels, while STEM allows simultaneous acquisition of high-resolution imaging and polarization states of individual unit cells. However, obtaining polarization distribution at the microscale remains challenging with TEM analyses. Moreover, sample preparation is destructive, and researchers should consider electron beam-induced artifacts such as irradiation damage, charging effects, and polarization shifts.

IV. Scattering Method

X-ray diffraction (XRD), based on scattering methods, provides insights into crystallography [150]. *In-situ* XRD has been employed to investigate both domain dynamics of relaxor-PT single crystals and the relationship between crystal structure and ferroelectric properties [151-153]. These studies have examined structural changes [39, 154-157], monoclinic phases [158-161], and domain dynamics such as polarization rotation [162] and AC poling effects [41, 163]. T. Li *et al.* conducted temperature-dependent synchrotron XRD to compare PZN-7PT and PZN-11PT, suggesting that the anomalous phase transition with monoclinic symmetry in PZN-7PT correlates with large dielectric and piezoelectric properties [155]. In another study, P. Finkel *et al.* utilized *in-situ* XRD to examine crystal structure upon mechanical stress and reveal structure-property relationships in 24PIN-PMN-30PT single crystals (Fig. 8) [161]. The (022) diffraction peak position exhibited hysteresis during stress application and removal, correlating with measured strain. At the (111) diffraction peak, two peaks merged into one when compressive stress exceeded ~35 MPa. Although hysteresis and phase transformation under mechanical loading can modify properties and domain structure [115, 164], systematic analysis of how performance actually decrease with pressure has been lacking. On the other hand. Qiu *et al.* used *in-situ* XRD to distinguish domain redistribution and domain wall motion under AC electric fields in PMN-26PT single crystals

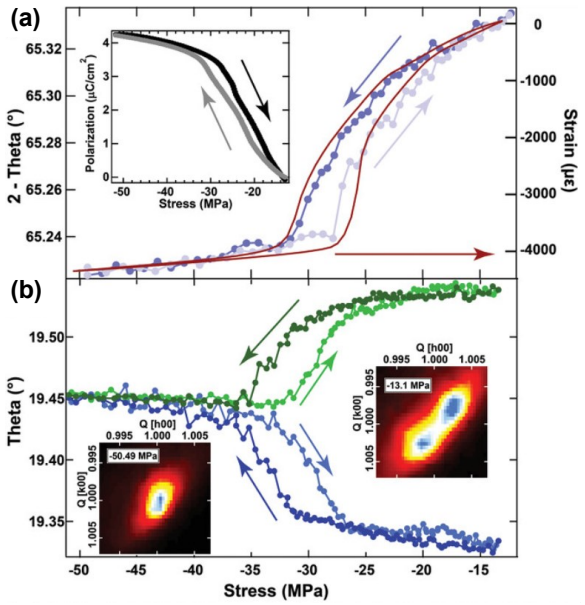

Fig. 8. Evolution of the (a) (220) and (b) (111) peaks during loading and unloading cycles. Also included in (a) is the stress-strain curve and the polarization in the inset. Reciprocal space map image plots for the (111) peak at low and high stress are shown as insets in (b). Note, the traditional engineering convention of compressive stress was adopted to be negative. The data reproduced with permission from [161].

[163]. In Fig. 9, AC electric fields eliminated two of the four domain variants by merging contiguous 71° ferroelectric domains, leading to increased domain size and a lamella structure with only 109° domains. Through domain and domain wall engineering, AC poling can enhance dielectric and piezoelectric properties compared to DC poling. However, recent studies present conflicting evidence, attributing improved extrinsic contributions to increased domain wall density [47, 85]. Moreover, it remains unclear why the presence of 71° domains results in decreased properties compared to samples containing only 109° domains. Significantly, small-signal measurements indicate more pronounced domain wall vibration in AC-poled samples, as evidenced by a higher peak at the phase transformation temperature compared to DC-poled samples. AC-poled samples can also exhibit a lower E_C than DC-poled samples, suggesting that AC poling produces materials with softer characteristics. Therefore, it would be misleading to assume that higher domain wall density always leads to greater domain wall motion and extrinsic contributions because of variations in domain wall orientation and alignment. To fully understand the mechanisms underlying improvements after AC poling, more comprehensive investigations are needed, particularly focusing on real-time domain dynamics and time-resolved studies.

Neutron methods can complement the limitations of XRD in *in-situ* analyses of ferroelectric materials [165], offering several advantages, including the absence of radiation damage and a large penetration depth of several centimeters. When studying complex oxides, sufficient scattering length can be generated between oxygen and other atoms [166], providing more accurate information about oxygen atomic positions

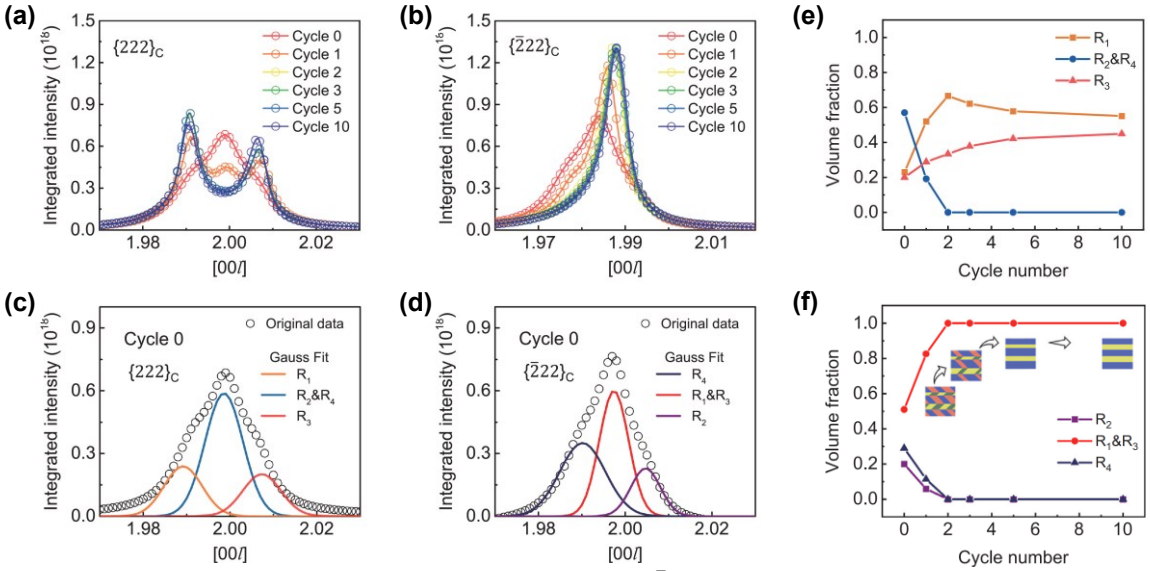

Fig. 9. (a), (b) Integrated intensity profiles along $[00l]_C$ direction for $\{222\}_C$ and $\{\bar{2}22\}_C$ reflections. (c), (d) Gauss fittings of the three peaks for the pristine PMN-26PT single crystal. (e), (f) The volume fractions of the four rhombohedral domain variants corresponding to the cycle number of AC electric field. The insets in (b) schematically illustrate the variation of domain structures. AC electric fields can merge the adjacent 71° ferroelectric domains to remove two of the four domain variants, thus creating lamellar structures with only 109° domains. The data reproduced with permission from [163].

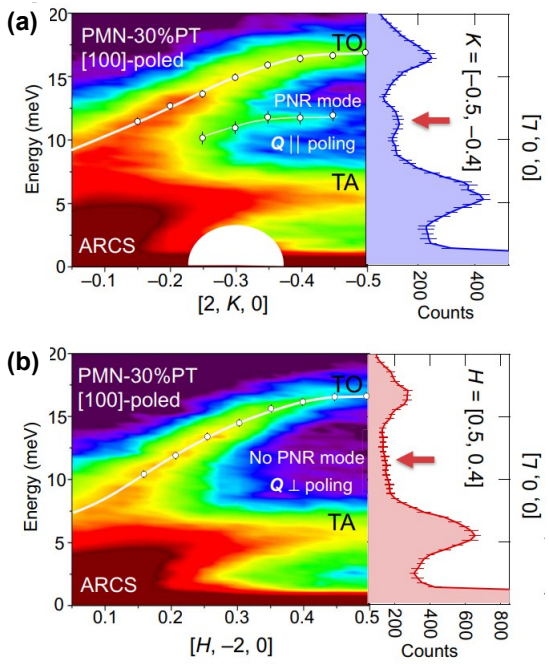

Fig. 10. Neutron scattering measurements of [100]-poled PMN-30PT at 300 K. (a) Phonon dispersion measured along reciprocal Q = [2, K, 0] (H = 2 ± 0.025 and L = 0 ± 0.025), where the PNR mode appears enhanced in this direction. (b) Phonon dispersion measured along reciprocal Q = [H, −2, 0] (K = −2 ± 0.025 and L = 0 ± 0.025), where PNR mode does not appear in this direction. The data reproduced with permission from [38].

compared to X-rays. Notably, displacement correlations in relaxor ferroelectrics manifest as polar nanoregions (PNRs) several nanometers in size [167-169]. Since cation disordering is accompanied by distortions of oxygen octahedra, many structural studies on relaxor ferroelectrics have employed neutron-based analyses, focusing on diffuse scattering patterns related to displacement correlations [168, 170-177]. Similarly, for relaxor-PT single crystals, neutron scattering has been used to study PNR dynamics and short-range correlated atomic displacements [36, 38, 178]. In Fig. 10, M. E. Manley *et al.* investigated the origin of high electromechanical coupling in [100]-poled PMN-30PT single crystals using neutron scattering [38]. Fig. 10(a) shows the PNR mode parallel to the poling direction, while no PNR mode perpendicular to the poling direction was detected in Fig. 10(b). This distinction in scattering patterns can be attributed to a low-energy soft phonon mode [68], which contributes to polarization rotation and giant piezoelectric properties. Additional studies have employed *in-situ* neutron diffraction to investigate domain dynamics and crystallography, including domain reorientation [179, 180], phase transformation [33, 181], and structural heterogeneity [182]. However, neutron methods require larger sample sizes, and neutron sources are less accessible than X-ray sources. Additionally, neutrons have a lower flux relative to photons, making time-resolved measurements more challenging.

X-ray Photon Correlation Spectroscopy (XPCS) can investigate the temporal evolution of structures and dynamics at the nanoscale [183]. In Fig. 11, the scattering can be measured through intensity changes scattered by a coherent incident X-ray beam over time [184]. Unlike other scattering methods, coherent X-rays produce a speckle pattern without averaging in the irradiated area. The time-dependent fluctuations of the speckle patterns can be examined using a two-time correlation function $C(t_1, t_2)$ [185]

$$C(t_1, t_2) = \left\langle \frac{\Delta I(Q, t_1)\, \Delta I(Q, t_2)}{\bar{I}(Q, t_1)\, \bar{I}(Q, t_2)} \right\rangle_Q, \qquad (2)$$

where $I(Q, t_i)$ is the intensity for wavevector Q at times t_i and $\Delta I(Q, t_i) \equiv I(Q, t_i) - \bar{I}(Q, t_i)$ is the deviation of intensity I in the speckle pattern from the mean intensity $\bar{I}$, which can be obtained under incoherent conditions where the speckle is not analyzed. $\bar{I}(Q, t_i)$ can be generated by smoothing $I(Q, t_i)$ across a range of detector areas, and <…> indicates the ensemble average over a range of Q with similar time

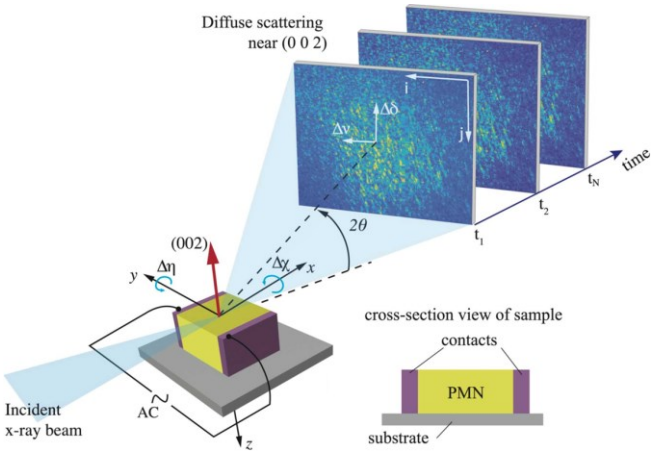

Fig. 11. Experimental setup of XPCS analyses showing vertical, nearly symmetric reflection scattering geometry and the coordinate axes. Inset is a cross-section view of relaxor ferroelectric PMN geometry and electrodes. The data reproduced with permission from [184].

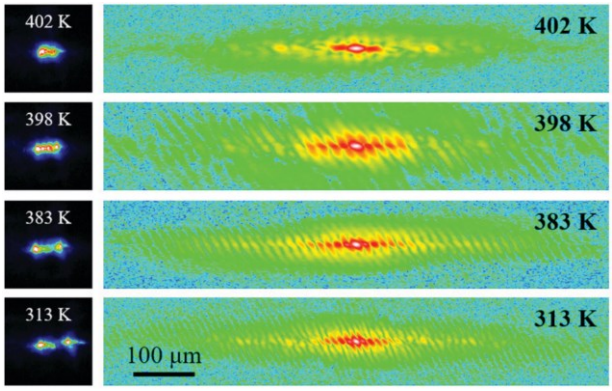

Fig. 12. Coherent soft X-ray radiation speckle patterns (left) and spatial correlation functions obtained from the speckle patterns (right) for the PMN-28PT single crystal measured under cooling in thermal equilibrium conditions. In the thermal equilibrium condition, the sample temperature was decreased by 0.2 K/min step and held for about 20 min before the speckle measurements. Cubic-to-tetragonal phase transformation took place at 407 K on cooling. The data reproduced with permission from [194].

correlations for normalization, ensuring that time variations in $\bar{I}$ do not contribute to the correlation function. XPCS is particularly well-suited for studying domain dynamics, as it can record speckle patterns with exposure and delay times shorter than the relaxation times, offering time resolution down to the microsecond range [186]. To date, XPCS has been applied to ferroelectric materials to investigate domain fluctuation [187, 188], phase transformations [189], and domain wall dynamics [190]. *In-situ* XPCS studies of relaxor ferroelectric single crystals have examined phase identification [191], polarization rotation [192], and domain size [193, 194]. In recent work, AC electric fields were applied during XPCS measurements to investigate domain dynamics in relaxor PMN single crystals [184]. The speckle correlation revealed responses AC fields, with PNRs in relaxor ferroelectrics contributing to spontaneous polarization and response to external electric fields. K. Namikawa *et al.* studied domain characteristics of [001]-cut PMN-28PT single crystals using coherent speckle techniques (Fig. 12) [194]. Their study observed irregularly shaped domains at 402 K, *i.e.*, just below the Curie point, that gradually evolved into stripe-shaped periodic domains as temperature decreased. The clear domain boundaries and narrower domain widths at lower temperatures suggest a large dielectric response to external electric fields. However, the piezoresponse induced by the X-ray beam can complicate XPCS interpretation [184], as results may be influenced by surface static charging of the irradiated area and electrostrictive properties. Therefore, it is essential to distinguish photon-induced properties from those caused by external stimuli. Furthermore, the equilibrium state should be ensured consistently to properly observe stimuli dependence [190]. Through enhanced understanding of time-resolved speckle patterns, XPCS will help address challenges regarding ferroelectric domains, particularly the relationship between domain dynamics and piezoelectricity in relaxor-PT single crystals.

V. Electromechanical Technique

Piezoresponse force microscopy (PFM) and its spectroscopy mode enable direct visualization and analysis of ferroelectric materials [195-198]. PFM measurements yield both amplitude and phase information; the amplitude represents voltage-induced deformation and strain, while phase reveals the relative polarization orientations of ferroelectric domains. Furthermore, both vertical (v-PFM) and lateral (l-PFM) measurements can be combined to construct three-dimensional vector domain structures. To date, researchers have been investigated domain dynamics of relaxor-PT single crystals via PFM, including nucleation and growth [199-203], domain switching phenomena [204-206], and phase transformations [35, 112, 207, 208]. For instance, K. Li et *al.* examined DC bias-induced domain switching in [001]-oriented PIN-PMN-38PT single crystals (Fig. 13) [202]. Under low bias stimulation (< 10 V), the nucleation and growth of 180° domains dominated during the switching process. However, as the electrical bias increased from 10 to 80 V, 90° domain switching gradually completed, achieving a single-domain state. These results indicated that switching behavior evolves with applied electric field strength: 180° domain switching is more sensitive at relatively lower electric fields, whereas non-180° domain switching becomes more dominant at higher electric field strengths, as confirmed by other studies [209, 210]. However, direct 180° polarization switching is generally considered difficult due to its high activation energy requirement and typically occurs through a combination of ferroelastic non-180° switching [211]. Therefore, carefully understanding and distinguishing domain switching orientations is crucial in ferroelectrics.

Regarding domain walls, both wall types and domain wall engineering have been studied via PFM. For example, Y. Jing *et al.* compared domain structures of $[011]_C$-poled rhombohedral PIN-PMN-PT and Mn-doped PIN-PMN-PT single crystals to explain the origin of internal bias (E_i) and large quality factor (Q_m), as shown in Fig. 14 [212]. Since rhombohedral single crystals have domain-engineered 2R with poling along the [011] direction [213, 214], the 2R domain structures can form through the arrangement of two spontaneous polarization (P_s) vectors. In undoped samples, when P_S vectors assemble head-to-tail, neutral domain walls

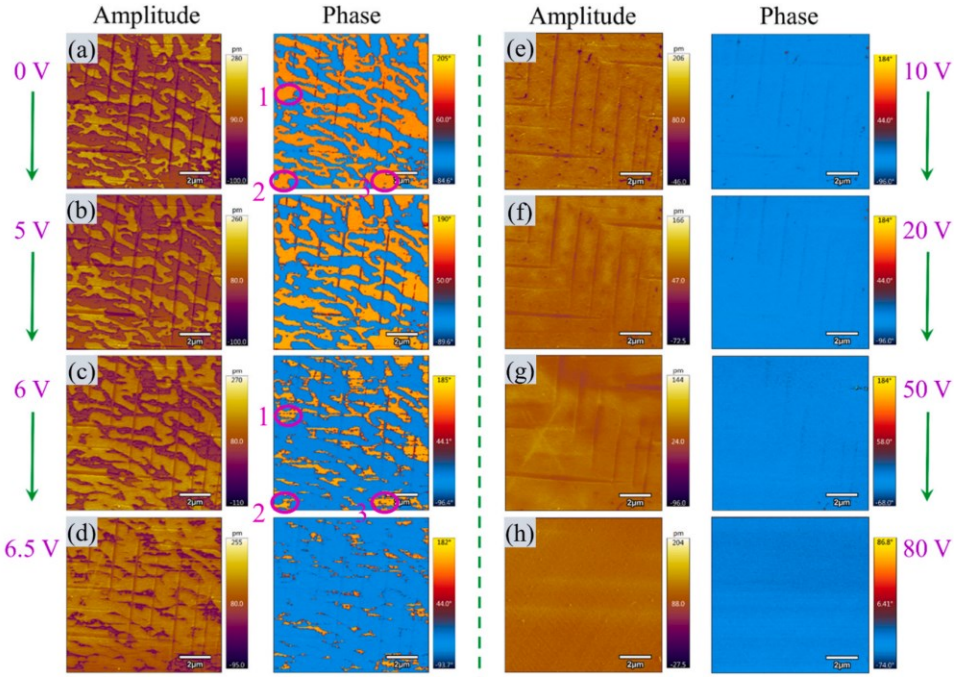

Fig. 13. (a)-(h) Domain evolution of PFM amplitude and phase images of $[001]_C$-oriented PIN-PMN-38PT single crystals with tetragonal phase at room temperature. The scanning area is 5 *μm* × 5 *μm* on the (001) plane, and the probe tip-bias direction is applied in the $[001]_C$ direction. The scanning rate in the writing and reading domain structure is fixed at a low frequency of 1 Hz. The data reproduced with permission from [202].

form parallel to the $(011)_C$ plane. However, in Mn-doped samples, P_S vectors connecting head-to-head/tail-to-tail create charged domain walls parallel to the $(001)_C$ plane. This suggests that Mn doping facilitates charged domain wall formation due to the presence of charged defects, such as negatively charged Mn^{2+}/Mn^{3+} and positively charged oxygen vacancies [27, 215-217]. Additionally, L. Yang *et al.* compared undoped and Mn-doped PIN-PMN-27PT single crystals using PFM, finding lower domain wall density in Mn-doped crystals [218]. This reduced density may contribute to decreased domain wall motion due to the pinning effect of defect dipoles. In PMN-34PT single crystals, neutral domain walls with lower domain wall energy were observed before poling, whereas DC bias can turn to charged domain walls between ferroelectric domain variants [219]. However, the distribution of charged domain walls may depend on several factors, including residual stress and defects. It is important to note that charged domain wall quantities can also vary between samples of the same nominal composition and within different areas of a given sample [220]. Although direct measurement of absolute domain wall density remains challenging, charged domain wall density in acceptor-doped or biased crystals typically exceeds that of virgin crystals [221-223]. From this perspective, the limited examples of domain structures related to donor doping effects suggest the need for further research in this area.

To date, the relationship between macroscopic properties and nanoscopic domain structures has been investigated through PFM imaging. Quantitative estimates of short-range polar order can be obtained using an autocorrelation function, $C(r)$, averaged over all in-plane directions

$$\langle C(r)\rangle = \sigma^2 \exp\left[-\left(\frac{r}{\xi}\right)^{2h}\right], \tag{3}$$

where r is the distance from the central peak, σ is a constant, ξ is the short-range correlation length, and h is the exponent parameter ($0 < h < 1$) [224, 225]. For example, W. He *et al.* demonstrated that PIN-PZ-PMN-PT single crystals exhibit enhanced thermal stabilities, where the smaller ξ value in the quaternary system, compared to binary PMN-20PT crystals, indicates a higher degree of relaxor behavior [226, 227]. The B-site cations, such as In^{3+} and Zr^{4+}, increase Pb-B repulsion and cation disordering in the ABO_3-lattice, leading to stronger relaxor properties [149, 228]. Similarly, X. Qi *et al.* compared undoped and Mn-doped PIN-PMN-29PT single crystals using an autocorrelation function, demonstrating that Mn doping suppresses the growth of PNRs within the ferroelectric phase [229]. Numerous studies have also examined AC poling through PFM analyses. Domain size emerges as a key factor in explaining the AC poling mechanism, with some research showing that decreased domain size and higher domain wall density correlate with improved properties [41, 43, 230, 231]. In contrast, other studies have demonstrated that AC poling enhances performance by increasing domain size and strengthening the domain contribution [50, 85, 232]. These conflicting results regarding domain size might stem from differences between the bulk and surface properties of samples. In PFM, images are generated from piezoelectric signals within an thin surface layer, approximately 10 nm depth [233]. Due to the skin effect in relaxor ferroelectrics [62, 234], domain patterns observed by PFM may differ from bulk structures and might not fully represent the macroscopic response. To address this limitation, researchers have integrated PFM analysis with simulation methods, particularly phase-field simulations, to verify nanodomain structures in relation to macroscopic dynamics [48, 50, 51, 235]. This integrated approach of experimental and simulation methods provides deeper insights into the overall domain behavior in relaxor-PT single crystals.

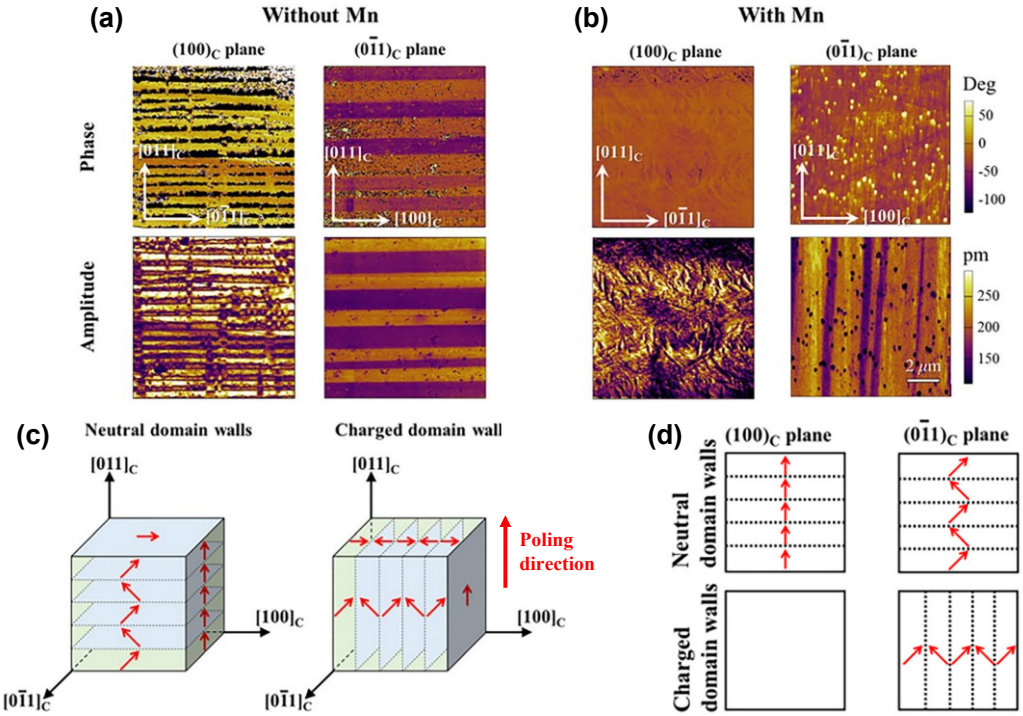

Fig. 14. The domain structures of $[011]_C$-poled PIN-PMN-PT and Mn-doped PIN-PMN-PT single crystals. The PFM amplitude and phase images observed on the $(100)_C$ and $(011)_C$ planes for (a) PIN-PMN-PT and (b) Mn-doped PIN-PMN-PT. Schematic 2R domain structures with neutral and charged domain walls (c) and their objections on $(100)_C$ and $(011)_C$ planes (d). The data reproduced with permission from [212].

VI. Conclusion

In this review, we detailed the complex relationship between ferroelectric domain dynamics and piezoelectricity in relaxor-PT single crystals. We clarified several challenging aspects from the literature, including monoclinic phase, field-induced phase transformation, polarization rotation, and PNRs. Through our review of experimental methods for studying domain dynamics, we have discussed both the strengths and limitations of various analytical approaches. It has become evident that domain dynamics can vary significantly across different analytic methods due to the inhomogeneous nature of domain configuration. Consequently, cross-validation using multiple techniques is essential for characterizing domain dynamics in relaxor-PT single crystals.

While experimental methods enable accurate measurement of domain dynamics, certain physical variables and mechanisms crucial to understanding properties remain unclear. Several challenges persist, and significant room exists for deeper understanding of domain dynamics, including the following:

(1) Distinguishing between domain and domain wall responses is important in ferroelectric dynamics. Domain contributions (including domain growth and orientation) and domain wall contributions (including domain wall motion and vibration) significantly influence properties, and further research from this perspective is necessary.

(2) The mechanism of AC poling remains unclear, with ongoing debates regarding domain size differences between AC and DC poling. This discrepancy may stem from inhomogeneous domain configurations and equipment limitations that inevitably create artifacts. To address this, time-resolved observations at suitable temporal and spatial scales are needed to enable more comprehensive investigation, particularly focusing on real-time domain dynamics.

(3) While poling studies are widespread, research on depoling processes remains limited. Although it is well established that temperature-induced depolarization of poled materials can alter domain configuration from preferred to random orientation, studies on electric field- or mechanical stress-induced depolarization in relaxor-PT single crystals are scarce. Systematic investigation of responses to electrical and mechanical stimuli is crucial for understanding practical applications.

Acknowledgment

This work was in part supported by NSF under grants # DMR 2011978 and DMR-2309184, and by ONR under Grant # N00014-21-1-2058.

References

[1] J. F. Scott and C. A. Paz de Araujo, "Ferroelectric memories," *Science*, vol. 246, no. 4936, pp. 1400-1405, Dec. 1989.

[2] J. Yu et al., "Hafnium-Based Ferroelectric Memory Device With Integrated Selective Function Using Crested Band Structure," *IEEE Trans. Electron Devices*, vol. 70, no. 10, pp. 5113-5118, Oct. 2023.

[3] K. S. Priya, S. Pal, M. Mohan, and P. Murugavel, "High Performance Near-Room-Temperature Pyroelectric Energy Harvesting Characteristics of Ferroelectric–Semiconductor Composites," *ACS Appl. Electron. Mater.*, vol. 5, no. 7, pp. 3790-3797, Jul. 2023.

[4] J. Li et al., "Grain-orientation-engineered multilayer ceramic capacitors for energy storage applications," *Nat. Mater.*, vol. 19, no. 9, pp. 999-1005, Sep. 2020.

[5] H. Pan et al., "Ultrahigh energy storage in superparaelectric relaxor ferroelectrics," *Science*, vol. 374, no. 6563, pp. 100-104, Oct. 2021.

[6] Y. R. Lee, T. Q. Trung, B. U. Hwang, and N. E. Lee, "A flexible artificial intrinsic-synaptic tactile sensory organ," *Nat. Commun.*, vol. 11, no. 1, p. 2753, Jun. 2020.

[7] J.-W. Sun et al., "Enhanced polarization retention and softening in [001]-oriented $Pb(Mg_{1/3}Nb_{2/3})$-$PbTiO_3$ single crystals through corona poling," *J. Korean Ceram. Soc.,* Apr. 2024.

[8] T. T. Zate et al., "Development of Textured 0.37 PMN-0.29 PIN-0.34 PT Ceramics-Based Multilayered Actuator for Cost-Effective Replacement of Single Crystal-Based Actuators," *J. Korean Inst. Electr. Electron. Mater. Eng.*, vol. 36, no. 4, pp. 362-368, Jul. 2023.

[9] W. Jo et al., "Giant electric-field-induced strains in lead-free ceramics for actuator applications–status and perspective," *J. Electroceram.*, vol. 29, pp. 71-93, Aug. 2012.

[10] M. N. Islam et al., "Boosting Piezoelectricity by 3D Printing PVDF-MoS_2 Composite as a Conformal and High-Sensitivity Piezoelectric Sensor," *Adv. Funct. Mater.*, vol. 33, no. 42, p. 2302946, Oct. 2023.

[11] S. Wu et al., "Cesium Lead Halide Perovskite Decorated Polyvinylidene Fluoride Nanofibers for Wearable Piezoelectric Nanogenerator Yarns," *ACS Nano*, vol. 17, no. 2, pp. 1022-35, Jan. 2023.

[12] X. Liu et al., "Ferroelectric crystals with giant electro-optic property enabling ultracompact Q-switches," *Science*, vol. 376, no. 6591, pp. 371-377, Apr. 2022.

[13] T. B. Xu et al., "Energy harvesting using a PZT ceramic multilayer stack,", *Smart Mater. Struct.*, vol. 22, no. 6, p. 065015, Jun. 2013.

[14] C. Peng, H. Wu, S. Kim, X. Dai, and X. Jiang, "Recent Advances in Transducers for Intravascular Ultrasound (IVUS) Imaging," *Sensors*, vol. 21, no. 10, p. 3540, May. 2021.

[15] A. R. Chowdhury, J. Jaksik, I. Hussain, P. Tran, S. Danti, and M. J. Uddin, "Surface-Modified Nanostructured Piezoelectric Device as a Cost-Effective Transducer for Energy and Biomedicine," *Energy Technol.*, vol. 7, no. 5, p. 1800767, May. 2019.

[16] S. E. Park and T. R. Shrout, "Ultrahigh strain and piezoelectric behavior in relaxor based ferroelectric single crystals," *J. Appl. Phys.*, vol. 82, no. 4, pp. 1804-1811, Aug. 1997.

[17] S. Zhang and F. Li, "High performance ferroelectric relaxor-$PbTiO_3$ single crystals: Status and perspective," *J. Appl. Phys.*, vol. 111, no. 3, p. 031301, Feb. 2012.

[18] E. Sun and W. Cao, "Relaxor-based ferroelectric single crystals: growth, domain engineering, characterization and applications," *Prog. Mater. Sci.*, vol. 65, pp. 124-210, Aug. 2014.

[19] Z.-G. Ye, B. Noheda, M. Dong, D. Cox, and G. Shirane, "Monoclinic phase in the relaxor-based piezoelectric/ferroelectric $Pb(Mg_{1/3}Nb_{2/3})O_3$-$PbTiO_3$ system," *Phys. Rev. B*, vol. 64, no. 18, p. 184114, Oct. 2001.

[20] J. M. Kiat, Y. Uesu, B. Dkhil, M. Matsuda, C. Malibert, and G. Calvarin, "Monoclinic structure of unpoled morphotropic high piezoelectric PMN-PT and PZN-PT compounds," *Phys. Rev. B*, vol. 65, no. 6, p. 064106, Feb. 2002.

[21] H. Liu et al., "Structural Evidence for Strong Coupling between Polarization Rotation and Lattice Strain in Monoclinic Relaxor Ferroelectrics," *Chem. Mat.*, vol. 29, no. 14, pp. 5767-5771, Jul. 2017.

[22] H.-P. Kim et al., "Symmetry-bridging phase as the mechanism for the large strains in relaxor-$PbTiO_3$ single crystals," *J. Eur. Ceram. Soc.*, vol. 39, no. 11, pp. 3327-3331, Sep. 2019.

[23] A. J. Bell, P. M. Shepley, and Y. Li, "Domain wall contributions to piezoelectricity in relaxor-lead titanate single crystals," *Acta Mater.*, vol. 195, pp. 292-303, Aug. 2020.

[24] A. Cui et al., "Designing Monoclinic Heterophase Coexistence for the Enhanced Piezoelectric Performance in Ternary Lead-Based Relaxor Ferroelectrics," *ACS Appl. Mater. Interfaces*, vol. 14, no. 8, pp. 10535-10545, Mar. 2022.

[25] H. Fu and R. E. Cohen, "Polarization rotation mechanism for ultrahigh electromechanical response in single-crystal piezoelectrics," *Nature*, vol. 403, no. 6767, pp. 281-283, Jan. 2000.

[26] B. Noheda, D. Cox, G. Shirane, S.-E. Park, L. Cross, and Z. Zhong, "Polarization rotation via a monoclinic phase in the piezoelectric 92% $PbZn_{1/3}Nb_{2/3}O_3$-8%$PbTiO_3$," *Phys. Rev. Lett.*, vol. 86, no. 17, p. 3891, Apr. 2001.

[27] S. Zhang, S.-M. Lee, D.-H. Kim, H.-Y. Lee, and T. R. Shrout, "Characterization of Mn-modified $Pb(Mg_{1/3}Nb_{2/3})O_3$–$PbZrO_3$–$PbTiO_3$ single crystals for high power broad bandwidth transducers," *Appl. Phys. Lett.*, vol. 93, no. 12, p. 122908, Sep. 2008.

[28] D. Damjanovic, "A morphotropic phase boundary system based on polarization rotation and polarization extension," *Appl. Phys. Lett.*, vol. 97, no. 6, p. 062906, Aug. 2010.

[29] X. Q. Huo et al., "Complete set of elastic, dielectric, and piezoelectric constants of $[011]_C$ poled rhombohedral $Pb(In_{0.5}Nb_{0.5})O_3$-$Pb(Mg_{1/3}Nb_{2/3})O_3$-$PbTiO_3$: Mn single crystals," *J. Appl. Phys.*, vol. 113, no. 7, p. 074106, Feb. 2013.

[30] L. Zheng, R. Sahul, S. Zhang, W. Jiang, S. Li, and W. Cao, "Orientation dependence of piezoelectric properties and mechanical quality factors of $0.27Pb(In_{1/2}Nb_{1/2})O_3$-$0.46Pb(Mg_{1/3}Nb_{2/3})O_3$-$0.27PbTiO_3$: Mn single crystals," *J. Appl. Phys.*, vol. 114, no. 10, p. 104105, Sep. 2013.

[31] B. Noheda, Z. Zhong, D. Cox, G. Shirane, S. Park, and P. Rehrig, "Electric-field-induced phase transitions in rhombohedral $Pb(Zn_{1/3}Nb_{2/3})_{1-x}Ti_xO_3$," *Phys. Rev. B*, vol. 65, no. 22, p. 224101, May 2002.

[32] J. Han and W. Cao, "Electric field effects on the phase transitions in [001]-oriented $(1-x)Pb(Mg_{1/3}Nb_{2/3})O_3-xPbTiO_3$ single crystals with compositions near the morphotropic phase boundary," *Phys. Rev. B*, vol. 68, no. 13, p. 134102, Oct. 2003.

[33] F. Bai et al., "X-ray and neutron diffraction investigations of the structural phase transformation sequence under electric field in $0.7Pb(Mg_{1/3}Nb_{2/3})$-$0.3PbTiO_3$ crystal," *J. Appl. Phys.*, vol. 96, no. 3, pp. 1620-1627, Aug. 2004.

[34] M. Davis, M. Budimir, D. Damjanovic, and N. Setter, "Rotator and extender ferroelectrics: Importance of the shear coefficient to the piezoelectric properties of domain-engineered crystals and ceramics," *J. Appl. Phys.*, vol. 101, no. 5, p. 054112, Mar. 2007.

[35] Q. Hu et al., "Nanoscale investigation on electric field induced ferroelectric phase transitions in the rhombohedral PMN-PT single crystal," *J. Alloy. Compd.*, vol. 953, p. 170118, Aug. 2023.

[36] G. Xu, J. Wen, C. Stock, and P. M. Gehring, "Phase instability induced by polar nanoregions in a relaxor ferroelectric system," *Nat. Mater.*, vol. 7, no. 7, pp. 562-566, Jul. 2008.

[37] F. Li et al., "The origin of ultrahigh piezoelectricity in relaxor-ferroelectric solid solution crystals," *Nat. Commun.*, vol. 7, no. 1, p. 13807, Dec. 2016.

[38] M. E. Manley et al., "Giant electromechanical coupling of relaxor ferroelectrics controlled by polar nanoregion vibrations," *Sci. Adv.*, vol. 2, no. 9, p. e1501814, Sep. 2016.

[39] G. Liu, L. P. Kong, Q. Y. Hu, and S. J. Zhang, "Diffused morphotropic phase boundary in relaxor-$PbTiO_3$ crystals: High piezoelectricity with improved thermal stability," *Appl. Phys. Rev.*, vol. 7, no. 2, p. 021405, Jun. 2020.

[40] X. Yao et al., "Structural evolution and ferroelectric properties of relaxor ferroelectric single crystal $Pb(Mg_{1/3}Nb_{2/3})O_3$-$0.28PbTiO_3$ under high pressure," *Appl. Phys. Lett.*, vol. 121, no. 3, p. 032901, Jul. 2022.

[41] W.-Y. Chang et al., "Dielectric and piezoelectric properties of $0.7Pb(Mg_{1/3}Nb_{2/3})O_3$-$0.3PbTiO_3$ single crystal poled using alternating current," *Mater. Res. Lett.*, vol. 6, no. 10, pp. 537-544, Oct. 2018.

[42] J. Xu et al., "Piezoelectric performance enhancement of $Pb(Mg_{1/3}Nb_{2/3})O_3$-$0.25PbTiO_3$ crystals by alternating current polarization for ultrasonic transducer," *Appl. Phys. Lett.*, vol. 112, no. 18, p. 182901, Apr. 2018.

[43] C. He, T. Karaki, X. Yang, Y. J. Yamashita, Y. Sun, and X. Long, "Dielectric and piezoelectric properties of $Pb[(Mg_{1/3}Nb_{2/3})_{0.52}(Yb_{1/2}Nb_{1/2})_{0.15}Ti_{0.33}]O_3$ single-crystal rectangular plate and beam mode transducers poled by alternate current poling," *Jpn. J. Appl. Phys.*, vol. 58, no. SL, p. SLLD06, Aug. 2019.

[44] L. Guo et al., "Orientation dependence of dielectric and piezoelectric properties of tetragonal relaxor ferroelectric single crystals by alternate current poling," *J. Appl. Phys.*, vol. 127, no. 18, p. 184104, May 2020.

[45] H. Wan, C. Luo, C.-C. Chung, Y. Yamashita, and X. Jiang, "Enhanced dielectric and piezoelectric properties of manganese-doped $Pb(In_{1/2}Nb_{1/2})O$-$Pb(Mg_{1/3}Nb_{2/3})O$-$PbTiO_3$ single crystals by alternating current poling," *Appl. Phys. Lett.*, vol. 118, no. 10, p. 102904, Mar. 2021.

[46] C. Luo, T. Karaki, Z. K. Wang, Y. Q. Sun, Y. Yamashita, and J. Y. Xu, "High piezoelectricity after field cooling AC poling in temperature stable ternary single crystals manufactured by continuous-feeding Bridgman method," *J. Adv. Ceram.*, vol. 11, no. 1, pp. 57-65, Jan. 2022.

[47] H. Hang, X. Jiang, D. Lin, F. Wang, and H. Luo, "Performance enhancements of $Pb(Mg_{1/3}Nb_{2/3})O_3$-$xPbTiO_3$ single crystal/epoxy 1–3 composite by alternating current polarization," *Curr. Appl. Phys.*, vol. 47, pp. 1-8, Mar. 2023.

[48] J. Liu et al., "Impact of alternating current electric field poling on piezoelectric and dielectric properties of $Pb(In_{1/2}Nb_{1/2})O_3$–$Pb(Mg_{1/3}Nb_{2/3})O_3$–$PbTiO_3$ ferroelectric crystals," *J. Appl. Phys.*, vol. 128, no. 9, p. 014108, Sep. 2020.

[49] C. Qiu et al., "Transparent ferroelectric crystals with ultrahigh piezoelectricity," *Nature*, vol. 577, no. 7790, pp. 350-354, Jan. 2020.

[50] H. Wan, C. Luo, C. Liu, W. Y. Chang, Y. Yamashita, and X. Jiang, "Alternating current poling on sliver-mode rhombohedral $Pb(Mg_{1/3}Nb_{2/3})O_3$-$PbTiO_3$ single crystals," *Acta Mater.*, vol. 208, p. 116759, Apr. 2021.

[51] B. Wang, F. Li, and L. Q. Chen, "Inverse Domain-Size Dependence of Piezoelectricity in Ferroelectric Crystals," *Adv. Mater.*, vol. 33, no. 51, p. 2105071, 2021.

[52] K. Song et al., "Enhanced piezoelectric properties and domain morphology under alternating current electric field poled in [001]-oriented PIN-PMN-PT single crystal," *J. Appl. Phys.*, vol. 132, no. 11, p. 114103, Sep. 2022.

[53] A. Negi et al., "Ferroelectric domain wall engineering enabled thermal modulation in PMN-PT single crystals," *Adv. Mater.*, vol. 35, no. 22, p. 2211286, Jun. 2023.

[54] F. Zavaliche et al., "Multiferroic $BiFeO_3$ films: domain structure and polarization dynamics," *Phase Transit.*, vol. 79, no. 12, pp. 991-1017, Dec. 2006.

[55] S. V. Kalinin, A. N. Morozovska, L. Q. Chen, and B. J. Rodriguez, "Local polarization dynamics in ferroelectric materials," *Rep. Prog. Phys.*, vol. 73, no. 5, p. 056502, May 2010.

[56] R. Xu et al., "Ferroelectric polarization reversal via successive ferroelastic transitions," *Nat. Mater.*, vol. 14, no. 1, pp. 79-86, Jan. 2015.

[57] L. Zheng et al., "Hysteretic phase transition sequence in $0.67Pb(Mg_{1/3}Nb_{2/3})O_3$–$0.33PbTiO_3$ single crystal driven by electric field and temperature," *Phys. Rev. B*, vol. 91, no. 18, p. 184105, May 2015.

[58] D. Zhu, X. Cheng, C. Yang, L. Shui, and Y. Li, "Direct observation of synchronized 90° domain switching in $BaTiO_3$ crystal during electric field loading," *Mater. Lett.*, vol. 282, p. 128706, Jan. 2021.

[59] H. Akamatsu et al., "Light-Activated Gigahertz Ferroelectric Domain Dynamics," *Phys. Rev. Lett.*, vol. 120, no. 9, p. 096101, Mar. 2018.

[60] H. J. Lee et al., "Electric-Field-Driven Nanosecond Ferroelastic-Domain Switching Dynamics in Epitaxial $Pb(Zr,Ti)O_3$ Film," *Phys. Rev. Lett.*, vol. 123, no. 21, p. 217601, Nov. 2019.

[61] J. Chrosch and E. K. H. Salje, "Near-surface domain structures in uniaxially stressed $SrTiO_3$," *J. Phys. Condens. Matter*, vol. 10, no. 13, pp. 2817-2827, Apr. 1998.

[62] G. Xu, P. Gehring, C. Stock, and K. Conlon, "The anomalous skin effect in single crystal relaxor ferroelectric PZN-x PT and PMN-x PT," *Phase Transit.*, vol. 79, no. 1-2, pp. 135-152, Jan. 2006.

[63] W. Ge et al., "Lead-free and lead-based ABO_3 perovskite relaxors with mixed-valence A-site and B-site disorder: Comparative neutron scattering structural study of $(Na_{1/2}Bi_{1/2})TiO_3$ and $Pb(Mg_{1/3}Nb_{2/3})O_3$," *Phys. Rev. B*, vol. 88, no. 17, p. 174115, Nov. 2013.

[64] N. Domingo, N. Bagués, J. Santiso, and G. Catalan, "Persistence of ferroelectricity above the Curie temperature at the surface of $Pb(Zn_{1/3}Nb_{2/3})O_3$−12%$PbTiO_3$," *Phys. Rev. B*, vol. 91, no. 9, p. 094111, Mar. 2015.

[65] A. A. Bokov and Z. G. Ye, "Domain structure in the monoclinic Pm phase of $Pb(Mg_{1/3}Nb_{2/3})O_3$–$PbTiO_3$ single crystals," *J. Appl. Phys.*, vol. 95, no. 11, pp. 6347-6359, Jun. 2004.

[66] C. Xu et al., "Domain Structure Evolutions During the Poling Process for [011]-Oriented PMN–xPT Crystals Across the MPB Region," *J. Am. Ceram. Soc.*, vol. 99, no. 6, pp. 2096-2102, Jun. 2016.

[67] L. Fan, J. Chen, Y. Ren, Z. Pan, L. Zhang, and X. Xing, "Unique Piezoelectric Properties of the Monoclinic Phase in $Pb(Zr,Ti)O_3$ Ceramics: Large Lattice Strain and Negligible Domain Switching," *Phys. Rev. Lett.*, vol. 116, no. 2, p. 027601, Jan. 2016.

[68] D. Hou et al., "Field-induced polarization rotation and phase transitions in $0.70Pb(Mg_{1/3}Nb_{2/3})O_3$–$0.30PbTiO_3$ piezoceramics observed by in situ high-energy x-ray scattering," *Phys. Rev. B*, vol. 97, no. 21, p. 214102, Jun. 2018.

[69] H. Liu et al., "Role of Reversible Phase Transformation for Strong Piezoelectric Performance at the Morphotropic Phase Boundary," *Phys. Rev. Lett.*, vol. 120, no. 5, p. 055501, Jan. 2018.

[70] M. E. Manley et al., "Phonon localization drives polar nanoregions in a relaxor ferroelectric," *Nat. Commun.*, vol. 5, no. 1, p. 3683, Apr. 2014.

[71] F. Li, S. Zhang, D. Damjanovic, L. Q. Chen, and T. R. Shrout, "Local Structural Heterogeneity and Electromechanical Responses of Ferroelectrics: Learning from Relaxor Ferroelectrics," *Adv. Funct. Mater.*, vol. 28, no. 37, p. 1801504, Sep. 2018.

[72] W. J. Merz, "Domain formation and domain wall motions in ferroelectric $BaTiO_3$ single crystals," *Phys. Rev.*, vol. 95, no. 3, p. 690, Aug. 1954.

[73] G. F. Nataf and M. Guennou, "Optical studies of ferroelectric and ferroelastic domain walls," *J. Phys. Condens. Matter*, vol. 32, no. 18, p. 183001, May 2020.

[74] J. Yao, Y. Yang, W. Ge, J. Li, and D. Viehland, "Domain evolution in $PbMg_{1/3}Nb_{2/3}O_3$–60at%$PbTiO_3$ with temperature and electric field," *J. Am. Ceram. Soc.*, vol. 94, no. 8, pp. 2479-2482, Aug. 2011.

[75] Z. Wang, R. Zhang, E. Sun, and W. Cao, "Temperature dependence of electric-field-induced domain switching in $0.7Pb(Mg_{1/3}Nb_{2/3})O_3$–$0.3PbTiO_3$ single crystal," *J. Alloy. Compd.*, vol. 527, pp. 101-105, Jun. 2012.

[76] X. Lu et al., "Temperature-dependent phase transition in $[001]_C$-oriented $0.72Pb(Mg_{1/3}Nb_{2/3})O_3$-$0.28PbTiO_3$ single crystals," *Ceram. Int.*, vol. 45, no. 11, pp. 13999-14005, Aug. 2019.

[77] J. Fan, X. Lu, and W. Cao, "Phase transitions and piezoelectricity enhancement around MC→O phase transition in PMN-0.34PT single crystals," *J. Alloy. Compd.*, vol. 835, p. 155171, Sep. 2020.

[78] X. Lu, J. Fan, H. Zhang, H. Wu, H. Li, and W. Cao, "Phase stability and Landau phenomenological model of relaxor ferroelectric single crystals $0.78Pb(Mg_{1/3}Nb_{2/3})O_3$-$0.22PbTiO_3$," *Ceram. Int.*, vol. 47, no. 7, pp. 9842-9848, Apr. 2021.

[79] F. Li, L. Wang, L. Jin, Z. Xu, and S. Zhang, "Achieving single domain relaxor-PT crystals by high temperature poling," *CrystEngComm*, vol. 16, no. 14, pp. 2892-2897, Jan. 2014.

[80] D. Lin, Z. Li, F. Li, and S. J. C. Zhang, "Direct observation of domain wall motion and novel dielectric loss in $0.23Pb(In_{1/2}Nb_{1/2})O_3$–$0.42Pb(Mg_{1/3}Nb_{2/3})O_3$–$0.35PbTiO_3$ crystals," *CrystEngComm*, vol. 15, no. 32, pp. 6292-6296, Jun. 2013.

[81] D. Lin et al., "In-situ observation of domain wall motion in $Pb(In_{1/2}Nb_{1/2})O_3$-$Pb(Mg_{1/3}Nb_{2/3})O_3$-$PbTiO_3$ crystals," *J. Appl. Phys.*, vol. 116, no. 3, Jul. 2014.

[82] X. Lu, H. Zhang, L. Zheng, and W. Cao, "Phase coexistence in ferroelectric solid solutions: Formation of monoclinic phase with enhanced piezoelectricity," *AIP Adv.*, vol. 6, no. 10, p. 105208, Oct. 2016.

[83] F. Li et al., "Giant piezoelectricity of Sm-doped $Pb(Mg_{1/3}Nb_{2/3})O_3$-$PbTiO_3$ single crystals," *Science*, vol. 364, no. 6437, pp. 264-268, Apr. 2019.

[84] A. M. Glazer, J. G. Lewis, and W. Kaminsky, "An automatic optical imaging system for birefringent media," *Proc. R. Soc. A*, vol. 452, no. 1955, pp. 2751-2765, Dec. 1996.

[85] C. Deng et al., "Reporting Excellent Transverse Piezoelectric and Electro-Optic Effects in Transparent Rhombohedral PMN-PT Single Crystal by Engineered Domains," *Adv. Mater.*, vol. 33, no. 43, p. e2103013, Oct. 2021.

[86] Z. Luo et al., "Meso- to nano-scopic domain structures in high Curie-temperature piezoelectric $BiScO_3$–$PbTiO_3$ single crystals of complex perovskite structure," *J. Mater. Chem. C*, vol. 8, no. 21, pp. 7234-7243, Apr. 2020.

[87] R. Oldenbourg and G. Mei, "New polarized light microscope with precision universal compensator," *J. Microsc.*, vol. 180, no. Pt 2, pp. 140-147, Nov. 1995.

[88] F. Massoumian, R. Juskaitis, M. A. Neil, and T. Wilson, "Quantitative polarized light microscopy," *J. Microsc.*, vol. 209, no. Pt 1, pp. 13-22, Jan. 2003.

[89] L. A. Pajdzik and A. M. Glazer, "Three-dimensional birefringence imaging with a microscope tilting-stage. I. Uniaxial crystals," *J. Appl. Crystallogr.*, vol. 39, no. 3, pp. 326-337, Jun. 2006.

[90] A. Kumar et al., "Probing mixed tetragonal/rhombohedral-like monoclinic phases in strained bismuth ferrite films by optical second harmonic generation," *Appl. Phys. Lett.*, vol. 97, no. 11, p. 112903, Sep. 2010.

[91] S. A. Denev, T. T. A. Lummen, E. Barnes, A. Kumar, and V. Gopalan, "Probing Ferroelectrics Using Optical Second Harmonic Generation," *J. Am. Ceram. Soc.*, vol. 94, no. 9, pp. 2699-2727, Sep. 2011.

[92] T. T. Lummen et al., "Thermotropic phase boundaries in classic ferroelectrics," *Nat. Commun.*, vol. 5, no. 1, p. 3172, Jan. 2014.

[93] T. T. Lummen et al., "Emergent Low-Symmetry Phases and Large Property Enhancements in Ferroelectric $KNbO_3$ Bulk Crystals," *Adv. Mater.*, vol. 29, no. 31, p. 1700530, Aug. 2017.

[94] J. Nordlander, G. De Luca, N. Strkalj, M. Fiebig, and M. Trassin, "Probing Ferroic States in Oxide Thin Films Using Optical Second Harmonic Generation," *Appl. Sci.*, vol. 8, no. 4, p. 570, Apr. 2018.

[95] Y. Zhang et al., "Characterization of domain distributions by second harmonic generation in ferroelectrics," *npj Comput. Mater.*, vol. 4, no. 1, p. 39, Jul. 2018.

[96] R. Xu et al., "Strain-induced room-temperature ferroelectricity in $SrTiO_3$ membranes," *Nat. Commun.*, vol. 11, no. 1, p. 3141, Jun. 2020.

[97] S. Reitzig, M. Rüsing, J. Zhao, B. Kirbus, S. Mookherjea, and L. M. Eng, "'Seeing is believing"—In-depth analysis by co-imaging of periodically-poled x-cut lithium niobate thin films," *Crystals*, vol. 11, no. 3, p. 288, Mar. 2021.

[98] W. Li et al., "Delineating complex ferroelectric domain structures via second harmonic generation spectral imaging," *J. Materiomics*, vol. 9, no. 2, pp. 395-402, Mar. 2023.

[99] X. Liu, S. Zhang, J. Luo, T. R. Shrout, and W. Cao, "Electric field dependence of nonlinearity parameters and third order elastic constants of $0.70Pb(Mg_{1/3}Nb_{2/3})O_3–0.30PbTiO_3$ single crystal," *Appl. Phys. Lett.*, vol. 96, no. 5, p. 052905, Feb. 2010.

[100] Y. Zhao et al., "Linear optical properties and second-harmonic generation of $(1-x)Pb(Mg_{1/3}Nb_{2/3})O_3–xPbTiO_3$ single crystals," *Ferroelectrics*, vol. 542, no. 1, pp. 112-119, Apr. 2019.

[101] X. Chen et al., "Quasi-phase matched second harmonic generation in a PMN-38PT crystal," *Opt. Lett.*, vol. 47, no. 8, pp. 2056-2059, Apr. 2022.

[102] J. Kaneshiro and Y. Uesu, "Domain structure analysis of $Pb(Zn_{1/3}Nb_{2/3})O_3–9\%PbTiO_3$ single crystals using optical second harmonic generation microscopy," *Phys. Rev. B*, vol. 82, no. 18, p. 184116, Nov. 2010.

[103] J. Kaneshiro and Y. Uesu, "SHG microscopic observation of $Pb(Zn_{1/3}Nb_{2/3})O_3–9\%PbTiO_3$ single crystal," *Phase Transit.*, vol. 84, no. 9-10, pp. 779-783, Sep. 2011.

[104] P. Tolédano, M. Guennou, and J. Kreisel, "Order-parameter symmetries of domain walls in ferroelectrics and ferroelastics," *Phys. Rev. B*, vol. 89, no. 13, p. 134104, Apr. 2014.

[105] H. Yokota, S. Matsumoto, E. K. H. Salje, and Y. Uesu, "Symmetry and three-dimensional anisotropy of polar domain boundaries observed in ferroelastic $LaAlO_3$ in the complete absence of ferroelectric instability," *Phys. Rev. B*, vol. 98, no. 10, p. 104105, Sep. 2018.

[106] F. Jiang and S. Kojima, "Raman scattering of $0.91Pb(Zn_{1/3}Nb_{2/3})O_3–0.09PbTiO_3$ relaxor ferroelectric single crystals," *Jpn. J. Appl. Phys.*, vol. 38, no. 9R, p. 5128, Sep. 1999.

[107] P. Lagos et al., "Identification of ferroelectric domain structures in $BaTiO_3$ for Raman spectroscopy," *Surf. Sci.*, vol. 532, pp. 493-500, Jun. 2003.

[108] M. Shen, G. Siu, Z. Xu, and W. Cao, "Raman spectroscopy study of ferroelectric modes in [001]-oriented $0.67Pb(Mg_{1/3}Nb_{2/3})O_3–0.33 PbTiO_3$ single crystals," *Appl. Phys. Lett.*, vol. 86, no. 25, p. 252903, Jun. 2005.

[109] Y. Yang et al., "Polarized Raman mapping study of the microheterogeneity in $0.67PbMg_{1/3}Nb_{2/3}O_3$-$0.33PbTiO_3$ single crystal," *J. Raman Spectrosc.*, vol. 41, no. 12, pp. 1735-1742, Dec. 2010.

[110] M. Rüsing et al., "Imaging of 180◦ ferroelectric domain walls in uniaxial ferroelectrics by confocal Raman spectroscopy: Unraveling the contrast mechanism," *Phys. Rev. Mater.*, vol. 2, no. 10, p. 103801, Oct. 2018.

[111] C. J. Chen et al., "Study of thermal and spatial dependent electric field-induced phase transition in relaxor ferroelectric crystals using Raman spectroscopy," *J. Alloy. Compd.*, vol. 804, pp. 35-41, Oct. 2019.

[112] Q. Hu et al., "Phase distribution and corresponding piezoelectric responses in a morphotropic phase boundary $Pb(Mg_{1/3}Nb_{2/3})O_3$-$PbTiO_3$ single crystal revealed by confocal Raman spectroscopy and piezo-response force microscopy," *J. Eur. Ceram. Soc.*, vol. 39, no. 14, pp. 4131-4138, Nov. 2019.

[113] Y. Yang et al., "Polarized micro-Raman study of the field-induced phase transition in the relaxor $0.67PbMg_{1/3}Nb_{2/3}O_3–0.33PbTiO_3$ single crystal," *Appl. Phys. Lett.*, vol. 95, no. 5, p. 051911, Aug. 2009.

[114] C. Chen et al., "Study of field-induced phase transitions in $0.68PbMg_{1/3}Nb_{2/3}O_3–0.32PbTiO_3$ relaxor single crystal by polarized micro-Raman spectroscopy," *Appl. Phys. Lett.*, vol. 105, no. 10, p. 102909, Sep. 2014.

[115] M. Ahart et al., "High-pressure Raman scattering and x-ray diffraction of the relaxor ferroelectric $0.96Pb(Zn_{1/3}Nb_{2/3})O_3–0.04PbTiO_3$," *Phys. Rev. B*, vol. 71, no. 14, p. 144102, Apr. 2005.

[116] S. Tsukada, Y. Fujii, A. Kanagawa, Y. Akishige, and K. Ohwada, "Polarization behavior in a compositionally graded relaxor–ferroelectric crystal visualized by angle-resolved polarized Raman mapping," *Commun. Phys.*, vol. 6, no. 1, p. 107, May 2023.

[117] C. R. Winkler, A. R. Damodaran, J. Karthik, L. W. Martin, and M. L. Taheri, "Direct observation of ferroelectric domain switching in varying electric field regimes using in situ TEM," *Micron*, vol. 43, no. 11, pp. 1121-1126, Nov. 2012.

[118] H. Guo et al., "Polarization alignment, phase transition, and piezoelectricity development in polycrystalline $0.5Ba(Zr_{0.2}Ti_{0.8})O_3$-$0.5(Ba_{0.7}Ca_{0.3})TiO_3$," *Phys. Rev. B*, vol. 90, no. 1, p. 014103, Jul. 2014.

[119] X. Liu, H. Guo, and X. Tan, "Evolution of structure and electrical properties with lanthanum content in $[(Bi_{1/2}Na_{1/2})_{0.95}Ba_{0.05}]_{1-x}La_xTiO_3$ ceramics," *J. Eur. Ceram. Soc.*, vol. 34, no. 12, pp. 2997-3006, Oct. 2014.

[120] H. Guo, X. Tan, and S. Zhang, "In situ TEM study on the microstructural evolution during electric fatigue in $0.7Pb(Mg_{1/3}Nb_{2/3})O_3–0.3PbTiO_3$ ceramic," *J. Mater. Res.*, vol. 30, no. 3, pp. 364-372, Feb. 2015.

[121] L. Li, J. R. Jokisaari, and X. Pan, "In situ electron microscopy of ferroelectric domains," *MRS Bull.*, vol. 40, no. 1, pp. 53-61, Jan. 2015.

[122] M. Zakhozheva et al., "Wide Compositional RangeIn SituElectric Field Investigations on Lead-Free $Ba(Zr_{0.2}Ti_{0.8})O_3–x(Ba_{0.7}Ca_{0.3})TiO_3$ Piezoceramic," *Phys. Rev. Appl.*, vol. 3, no. 6, p. 064018, Jun. 2015.

[123] Z. M. Fan, J. Koruza, J. Rödel, and X. L. Tan, "An ideal amplitude window against electric fatigue in $BaTiO_3$-based lead-free piezoelectric materials," *Acta Mater.*, vol. 151, pp. 253-259, Jun. 2018.

[124] T. Sumigawa et al., "TEM observation of nanodomain mechanics in barium titanate under external loads," *Phys. Rev. Mater.*, vol. 4, no. 5, p. 054415, May 2020.

[125] U. Belegundu, X. Du, A. Bhalla, and K. Uchino, "Effect of electric field on domain formation in relaxor based $Pb(Zn_{1/3}Nb_{2/3})O_3$-$PbTiO_3$ single crystals," *Ferroelectr. Lett. Sect.*, vol. 26, no. 5-6, pp. 107-116, Dec. 1999.

[126] X. Tan, Z. Xu, J. Shang, and P. Han, "Direct observations of electric field-induced domain boundary cracking in <001> oriented piezoelectric $Pb(Mg_{1/3}Nb_{2/3})O_3–PbTiO_3$ single crystal," *Appl. Phys. Lett.*, vol. 77, no. 10, pp. 1529-1531, Sep. 2000.

[127] Y. Sato, T. Hirayama, and Y. Ikuhara, "Real-time direct observations of polarization reversal in a piezoelectric crystal: $Pb(Mg_{1/3}Nb_{2/3})O_3–PbTiO_3$ studied via in situ electrical biasing transmission electron microscopy," *Phys. Rev. Lett.*, vol. 107, no. 18, p. 187601, Oct. 2011.

[128] Y. Sato, T. Hirayama, and Y. Ikuhara, "Evolution of nanodomains under DC electrical bias in $Pb(Mg_{1/3}Nb_{2/3})O_3$-$PbTiO_3$: An in-situ transmission electron microscopy study," *Appl. Phys. Lett.*, vol. 100, no. 17, p. 172902, Apr. 2012.

[129] Q. Huang et al., "Direct observation of nanoscale dynamics of ferroelectric degradation," *Nat. Commun.*, vol. 12, no. 1, p. 2095, Apr. 2021.

[130] Z. Chen et al., "Facilitation of Ferroelectric Switching via Mechanical Manipulation of Hierarchical Nanoscale Domain Structures," *Phys. Rev. Lett.*, vol. 118, no. 1, p. 017601, Jan. 2017.

[131] Z. Chen, Q. Huang, F. Wang, S. P. Ringer, H. Luo, and X. Liao, "Stress-induced reversible and irreversible ferroelectric domain switching," *Appl. Phys. Lett.*, vol. 112, no. 15, p. 152901, Apr. 2018.

[132] Y. Liu, J. Xia, P. Finkel, S. D. Moss, X. Liao, and J. M. Cairney, "Real-time observation of stress-induced domain evolution in a [011] PIN-PMN-PT relaxor ferroelectric single crystal," *Acta Mater.*, vol. 175, pp. 436-444, Aug. 2019.

[133] F. Chu, I. M. Reaney, and N. Setter, "Role of Defects in the Ferroelectric Relaxor Lead Scandium Tantalate," *J. Am. Ceram. Soc.*, vol. 78, no. 7, pp. 1947-1952, Jul. 2005.

[134] R. C. Smith and C. L. Hom, "Domain wall theory for ferroelectric hysteresis," *J. Intell. Mater. Syst. Struct.*, vol. 10, no. 3, pp. 195-213, Mar. 1999.

[135] Y. Nahas, S. Prokhorenko, I. Kornev, and L. Bellaiche, "Topological Point Defects in Relaxor Ferroelectrics," *Phys. Rev. Lett.*, vol. 116, no. 12, p. 127601, Mar. 2016.

[136] K. Sato and N. Asakura, "Domain switching dynamics in relaxor ferroelectric $Pb(Mg_{1/3}Nb_{2/3})O_3–PbTiO_3$ revealed by time-resolved high-voltage electron microscopy," *J. Appl. Phys.*, vol. 130, no. 16, p. 164101, Oct. 2021.

[137] C. L. Jia, K. W. Urban, M. Alexe, D. Hesse, and I. Vrejoiu, "Direct observation of continuous electric dipole rotation in flux-closure domains in ferroelectric $Pb(Zr,Ti)O_3$," *Science*, vol. 331, no. 6023, pp. 1420-3, Mar. 2011.

[138] C. T. Nelson et al., "Spontaneous Vortex Nanodomain Arrays at Ferroelectric Heterointerfaces," *Nano Lett.*, vol. 11, no. 2, pp. 828-834, Feb. 2011.

[139] P. Gao et al., "Atomic-scale mechanisms of ferroelastic domain-wall-mediated ferroelectric switching," *Nat. Commun.*, vol. 4, no. 1, p. 2791, Nov. 2013.

[140] A. Yadav et al., "Observation of polar vortices in oxide superlattices," *Nature*, vol. 530, no. 7589, pp. 198-201, Feb. 2016.

[141] Y. Zhang et al., "Deterministic Ferroelastic Domain Switching Using Ferroelectric Bilayers," *Nano Lett.*, vol. 19, no. 8, pp. 5319-5326, Aug. 2019.

[142] C. T. Nelson et al., "Exploring physics of ferroelectric domain walls via Bayesian analysis of atomically resolved STEM data," *Nat. Commun.*, vol. 11, no. 1, p. 6361, Dec. 2020.

[143] S. Lindemann et al., "Low-voltage magnetoelectric coupling in membrane heterostructures," *Sci. Adv.*, vol. 7, no. 46, p. eabh2294, Nov. 2021.

[144] K. Moore, U. Bangert, and M. Conroy, "Aberration corrected STEM techniques to investigate polarization in ferroelectric domain walls and vortices," *APL Mater.*, vol. 9, no. 2, p. 020703, Feb. 2021.

[145] Z. Chen et al., "Giant tuning of ferroelectricity in single crystals by thickness engineering," *Sci. Adv.*, vol. 6, no. 42, p. eabc7156, Oct. 2020.

[146] A. Kumar et al., "Atomic-resolution electron microscopy of nanoscale local structure in lead-based relaxor ferroelectrics," *Nat. Mater.*, vol. 20, no. 1, pp. 62-67, Jan. 2021.

[147] Y. Liu, R.-M. Niu, S. D. Moss, P. Finkel, X.-Z. Liao, and J. M. Cairney, "Atomic coordinates and polarization map around a pair of $\frac{1}{2}a[01\bar{1}]$ dislocation cores produced by plastic deformation in relaxor ferroelectric PIN–PMN–PT," *J. Appl. Phys.*, vol. 129, no. 23, p. 234101, Jun. 2021.

[148] R. Wang et al., "Ferroelectric domain structure and atomic-scale phase distribution in a $Pb(Mg_{1/3}Nb_{2/3})O_3$-$PbTiO_3$ single crystal," *Ceram. Int.*, vol. 48, no. 3, pp. 3869-3874, Feb. 2022.

[149] L. Yang et al., "Simultaneously achieving giant piezoelectricity and record coercive field enhancement in relaxor-based ferroelectric crystals," *Nat. Commun.*, vol. 13, no. 1, p. 2444, May 2022.

[150] S. Gorfman, "Sub-microsecond X-ray crystallography: techniques, challenges, and applications for materials science," *Crystallogr. Rev.*, vol. 20, no. 3, pp. 210-232, Jul. 2014.

[151] J. J. Zhu, W. W. Li, G. S. Xu, K. Jiang, Z. G. Hu, and J. H. Chu, "A phenomenological model of electronic band structure in ferroelectric $Pb(In_{1/2}Nb_{1/2})O_3$–$Pb(Mg_{1/3}Nb_{2/3})O_3$–$PbTiO_3$ single crystals around the morphotropic phase boundary determined by temperature-dependent transmittance spectra," *Acta Mater.*, vol. 59, no. 17, pp. 6684-6690, Oct. 2011.

[152] N. Luo et al., "PMN-PT based quaternary piezoceramics with enhanced piezoelectricity and temperature stability," *Appl. Phys. Lett.*, vol. 104, no. 18, p. 182911, May 2014.

[153] Y. Zhang, H. Liu, S. Sun, S. Deng, and J. Chen, "Systematic study of structure and piezoelectric properties of $Pb(Ni_{1/3}Nb_{2/3})O_3$-$PbTiO_3$ by in situ synchrotron diffraction," *J. Am. Ceram. Soc.*, vol. 104, no. 1, pp. 604-612, Jan. 2020.

[154] J. Xiao, X. Zhang, P. Zhu, W. Huang, and Q. Yuan, "Synchrotron radiation topography study of temperature-induced phase transformation in unpoled $0.92Pb(Zn_{1/3}Nb_{2/3})O_3$–$0.08PbTiO_3$ crystals," *Solid State Commun.*, vol. 148, no. 3-4, pp. 109-112, Oct. 2008.

[155] T. Li et al., "Ferroelastic domain structure and phase transition in single-crystalline $[PbZn_{1/3}Nb_{2/3}O_3]_{1-x}[PbTiO_3]_x$ observed via in-situ x-ray microbeam," *J. Eur. Ceram. Soc.*, vol. 38, no. 4, pp. 1488-1497, Apr. 2018.

[156] Y. Wang et al., "Temperature-induced and electric-field-induced phase transitions in rhombohedral $Pb(In_{1/2}Nb_{1/2})O_3$–$Pb(Mg_{1/3}Nb_{2/3})O3$–$PbTiO_3$ ternary single crystals," *Phys. Rev. B*, vol. 90, no. 13, p. 134107, Oct. 2014.

[157] J.-W. Sun et al., "Understanding thermal depolarization via thermally stimulated depolarization current measurement," *J. Korean Ceram. Soc.*, vol. 61, p. 654–660, Apr. 2024.

[158] Y. Kitanaka et al., "Synchrotron radiation analyses of lattice strain behaviors for rhombohedral $Pb(Zn_{1/3}Nb_{2/3})O_3$–$PbTiO_3$ single crystals under electric fields," *J. Ceram. Soc. Jpn.*, vol. 121, no. 1416, pp. 632-637, Aug. 2013.

[159] S. V. Rajasekaran, S. N. Achary, S. J. Patwe, R. Jayavel, G. Mangamma, and A. K. Tyagi, "Phase transformation in relaxor-ferroelectric single crystal $[Pb(Sc_{1/2}Nb_{1/2})O_3]_{0.58}$–$[PbTiO_3]_{0.42}$," *J. Mater. Res.*, vol. 29, no. 9, pp. 1054-1061, May 2014.

[160] Y. Wang, G. Yuan, H. Luo, J. Li, and D. Viehland, "Phase transition in the near-surface region of ternary $Pb(In_{1/2}Nb_{1/2})O_3$–$Pb(Mg_{1/3}Nb_{2/3})O_3$–$PbTiO_3$ relaxor ferroelectric crystals," *Phys. Rev. Appl.*, vol. 8, no. 3, p. 034032, Sep. 2017.

[161] P. Finkel et al., "Simultaneous Large Optical and Piezoelectric Effects Induced by Domain Reconfiguration Related to Ferroelectric Phase Transitions," *Adv. Mater.*, vol. 34, no. 7, p. e2106827, Feb. 2022.

[162] S. Aoyagi et al., "Time-Resolved Nanobeam X-ray Diffraction of a Relaxor Ferroelectric Single Crystal under an Alternating Electric Field," *Crystals*, vol. 11, no. 11, p. 1419, Nov. 2021.

[163] C. Qiu et al., "In-situ domain structure characterization of $Pb(Mg_{1/3}Nb_{2/3})O_3$-$PbTiO_3$ crystals under alternating current electric field poling," *Acta Mater.*, vol. 210, p. 116853, May 2021.

[164] E. A. Patterson et al., "Dynamic piezoelectric response of relaxor single crystal under electrically driven inter-ferroelectric phase transformations," *Appl. Phys. Lett.*, vol. 116, no. 22, p. 222903, Jun. 2020.

[165] G. Esteves, C. M. Fancher, and J. L. Jones, "In situ characterization of polycrystalline ferroelectrics using x-ray and neutron diffraction," *J. Mater. Res.*, vol. 30, no. 3, pp. 340-356, Feb. 2014.

[166] M. Yashima, "observations of phase transition using high-temperature neutron and synchrotron X-ray powder diffractometry," *J. Am. Ceram. Soc.*, vol. 85, no. 12, pp. 2925-2930, Dec. 2002.

[167] G. Burns and F. H. Dacol, "Glassy polarization behavior in ferroelectric compounds and," *Solid State Commun.*, vol. 48, no. 10, pp. 853-856, Dec. 1983.

[168] H. Hiraka, S. H. Lee, P. M. Gehring, G. Xu, and G. Shirane, "Cold neutron study on the diffuse scattering and phonon excitations in the relaxor $Pb(Mg_{1/3}Nb_{2/3})O_3$," *Phys. Rev. B*, vol. 70, no. 18, p. 184105, Nov. 2004.

[169] R. A. Cowley, S. N. Gvasaliya, S. G. Lushnikov, B. Roessli, and G. M. Rotaru, "Relaxing with relaxors: a review of relaxor ferroelectrics," *Adv. Phys.*, vol. 60, no. 2, pp. 229-327, Apr. 2011.

[170] A. Naberezhnov, S. Vakhrushev, B. Dorner, D. Strauch, and H. Moudden, "Inelastic neutron scattering study of the relaxor ferroelectric $PbMg_{1/3}Nb_{2/3}O_3$ at high temperatures," *Eur. Phys. J. B*, vol. 11, no. 1, pp. 13-20, Sep. 1999.

[171] I. K. Jeong et al., "Direct observation of the formation of polar nanoregions in $Pb(Mg_{1/3}Nb_{2/3})O_3$ using neutron pair distribution function analysis," *Phys. Rev. Lett.*, vol. 94, no. 14, p. 147602, Apr. 2005.

[172] S. Vakhrushev, A. Ivanov, and J. Kulda, "Diffuse neutron scattering in relaxor ferroelectric $PbMg_{1/3}Nb_{2/3}O_3$," *Phys. Chem. Chem. Phys.*, vol. 7, no. 11, pp. 2340-2345, Jun. 2005.

[173] P. M. Gehring et al., "Reassessment of the Burns temperature and its relationship to the diffuse scattering, lattice dynamics, and thermal expansion in relaxor $Pb(Mg_{1/3}Nb_{2/3})O_3$," *Phys. Rev. B*, vol. 79, no. 22, p. 224109, Jun. 2009.

[174] A. Bosak, D. Chernyshov, S. Vakhrushev, and M. Krisch, "Diffuse scattering in relaxor ferroelectrics: true three-dimensional mapping, experimental artefacts and modelling," *Acta Crystallogr. Sect. A*, vol. 68, no. Pt 1, pp. 117-123, Jan. 2012.

[175] M. Paściak, T. R. Welberry, J. Kulda, M. Kempa, and J. Hlinka, "Polar nanoregions and diffuse scattering in the relaxor ferroelectric $PbMg_{1/3}Nb_{2/3}O_3$," *Phys. Rev. B*, vol. 85, no. 22, p. 224109, Jun. 2012.

[176] M. J. Krogstad et al., "The relation of local order to material properties in relaxor ferroelectrics," *Nat. Mater.*, vol. 17, no. 8, pp. 718-724, Aug. 2018.

[177] M. Eremenko et al., "Local atomic order and hierarchical polar nanoregions in a classical relaxor ferroelectric," *Nat. Commun.*, vol. 10, no. 1, p. 2728, Jun. 2019.

[178] Z. Xu, J. Wen, E. Mamontov, C. Stock, P. M. Gehring, and G. Xu, "Freezing of the local dynamics in the relaxor ferroelectric $[Pb(Zn_{1/3}Nb_{2/3})O_3]_{0.955}[PbTiO_3]_{0.045}$," *Phys. Rev. B*, vol. 86, no. 14, p. 144106, Oct. 2012.

[179] J. E. Daniels et al., "Neutron diffraction study of the polarization reversal mechanism in $[111]_C$-oriented $Pb(Zn_{1/3}Nb_{2/3})O_3$–$xPbTiO_3$," *J. Appl. Phys.*, vol. 101, no. 10, p. 104108, May. 2007.

[180] A. Pramanick, A. D. Stoica, and K. An, "High-resolution 2-D Bragg diffraction reveal heterogeneous domain transformation behavior in a bulk relaxor ferroelectric," *Appl. Phys. Lett.*, vol. 109, no. 9, p. 092907, Aug. 2016.

[181] Q. Li et al., "In-situ neutron diffraction study of $Pb(In_{1/2}Nb_{1/2})O_3$-$Pb(Mg_{1/3}Nb_{2/3})O_3$-$PbTiO_3$ single crystals under uniaxial mechanical stress," *J. Appl. Phys.*, vol. 111, no. 8, p. 084110, Apr. 2012.

[182] Y. Lu et al., "Giant piezoelectric response in Ho-doped $PbMg_{1/3}Nb_{2/3}TiO_3$ relaxor ferroelectric single crystals via in-situ neutron scattering," *Mater. Today Adv.*, vol. 17, p. 100345, Mar. 2023.

[183] A. R. Sandy, Q. Zhang, and L. B. Lurio, "Hard X-Ray Photon Correlation Spectroscopy Methods for Materials Studies," *Annu. Rev. Mater. Res.*, Vol 48, vol. 48, pp. 167-190, Jul. 2018.

[184] D. Sheyfer et al., "X-ray-induced piezoresponse during X-ray photon correlation spectroscopy of $PbMg_{1/3}Nb_{2/3}O_3$," *J. Synchrot. Radiat.*, vol. 31, no. 1, pp. 55-64, Jan. 2024.

[185] O. Bikondoa, "On the use of two-time correlation functions for X-ray photon correlation spectroscopy data analysis," *J. Appl. Crystallogr.*, vol. 50, no. Pt 2, pp. 357-368, Apr. 2017.

[186] A. Madsen, A. Fluerasu, and B. Ruta, "Structural dynamics of materials probed by X-ray photon correlation spectroscopy," in *Synchrotron Light Sources and Free-Electron Lasers*, pp. 1989-2018, May. 2020.

[187] Q. Zhang et al., "Thermal fluctuations of ferroelectric nanodomains in a ferroelectric-dielectric $PbTiO_3$/$SrTiO_3$ superlattice," *Phys. Rev. Lett.*, vol. 118, no. 9, p. 097601, Feb. 2017.

[188] J. Li et al., "Domain fluctuations in a ferroelectric low-strain $BaTiO_3$ thin film," *Phys. Rev. Mater.*, vol. 4, no. 11, p. 114409, Nov. 2020.

[189] N. Oshime et al., "Lattice strain visualization inside a 400 nm single grain of $BaTiO_3$ in polycrystalline ceramics by Bragg coherent X-ray diffraction imaging," *Jpn. J. Appl. Phys.*, vol. 62, no. Sm, p. SM1022, Nov. 2023.

[190] S. Gorfman et al., "Ferroelectric domain wall dynamics characterized with X-ray photon correlation spectroscopy," *Proc. Natl. Acad. Sci.*, vol. 115, no. 29, pp. E6680-E6689, Jul. 2018.

[191] L. Cai, R. Pattnaik, J. Lundeen, and J. Toulouse, "Piezoelectric polar nanoregions and relaxation-coupled resonances in relaxor ferroelectrics," *Phys. Rev. B*, vol. 98, no. 13, p. 134113, Oct. 2018.

[192] K. Ohwada et al., "Polarization rotation associated with phonon dynamics in monoclinic C phase near morphotropic phase boundary studied by diffuse and inelastic X-ray scattering from a Ti-composition-gradient $Pb[(Mg_{1/3}Nb_{2/3})_{1-x}Ti_x]O_3$ single crystal," *Ferroelectrics*, vol. 532, no. 1, pp. 100-110, Aug. 2018.

[193] D. Shimizu et al., "Negative correlation between electrical response and domain size in a Ti-composition-gradient $Pb[(Mg_{1/3}Nb_{2/3})_{1-x}Ti_x]O_3$ crystal near the morphotropic phase boundary," *Phys. Rev. B*, vol. 92, no. 17, p. 174121, Nov. 2015.

[194] K. Namikawa et al., "Mesoscopic hierarchic polarization structure in the relaxor ferroelectrics $Pb[(Mg_{1/3}Nb_{2/3})_{1-x}Ti_x]O_3$," *Phys. Rev. B*, vol. 100, no. 18, p. 184110, Nov. 2019.

[195] N. Balke, I. Bdikin, S. V. Kalinin, and A. L. Kholkin, "Electromechanical Imaging and Spectroscopy of Ferroelectric and Piezoelectric Materials: State of the Art and Prospects for the Future," *J. Am. Ceram. Soc.*, vol. 92, no. 8, pp. 1629-1647, Aug. 2009.

[196] S. Jesse, A. P. Baddorf, and S. V. Kalinin, "Switching spectroscopy piezoresponse force microscopy of ferroelectric materials," *Appl. Phys. Lett.*, vol. 88, no. 6, p. 062908, Feb. 2006.

[197] S. V. Kalinin, A. Rar, and S. Jesse, "A decade of piezoresponse force microscopy: progress, challenges, and opportunities," *IEEE Trans. Ultrason. Ferroelectr. Freq. Control*, vol. 53, no. 12, pp. 2226-2252, Dec. 2006.

[198] T. Li and K. Zeng, "Probing of Local Multifield Coupling Phenomena of Advanced Materials by Scanning Probe Microscopy Techniques," *Adv. Mater.*, vol. 30, no. 47, p. e1803064, Nov. 2018.

[199] W.-Y. Chang et al., "Patterned nano-domains in PMN-PT single crystals," *Acta Mater.*, vol. 143, pp. 166-173, Jan. 2018.

[200] R. Gainutdinov, Y. V. Bodnarchuk, T. Volk, X. Wei, and X. Liu, "AFM-tip written normal and anomalous domains in PMN-0.4PT crystals," *J. Appl. Phys.*, vol. 126, no. 2, p. 024101, Jul. 2019.

[201] K. Li et al., "Observation of Micro-Scale Domain Structure Evolution under Electric Bias in Relaxor-Based PIN-PMN-PT Single Crystals," *Crystals*, vol. 13, no. 11, p. 1599, Nov. 2023.

[202] K. Li et al., "Multi-type nanoscale domain switching dynamics in tetragonal PIN-PMN-PT single crystal under electrical bias," *Ceram. Int.*, vol. 49, no. 1, pp. 109-116, Jan. 2023.

[203] Q. Li, Y. Liu, R. L. Withers, Y. H. Wan, Z. R. Li, and Z. Xu, "Piezoresponse force microscopy studies on the domain structures and local switching behavior of $Pb(In_{1/2}Nb_{1/2})O_3$-$Pb(Mg_{1/3}Nb_{2/3})O_3$-$PbTiO_3$ single crystals," *J. Appl. Phys.*, vol. 112, no. 5, Sep. 2012.

[204] D. Zhang, L. Wang, L. Li, P. Sharma, and J. Seidel, "Varied domain structures in $0.7Pb(Mg_{1/3}Nb_{2/3})O_3$-$0.3PbTiO_3$ single crystals," *Microstructures*, vol. 3, no. 4, p. 2023046, Dec. 2023.

[205] Y. Ming et al., "Orientation dependence of polarization-modulated photovoltaic effect of relaxor-based $Pb(In_{1/2}Nb_{1/2})O_3$–$Pb(Mg_{1/3}Nb_{2/3})O_3$–$PbTiO_3$ single crystals," *J. Alloy. Compd.*, vol. 902, p. 163777, May 2022.

[206] J. Bian et al., "Fingerprints of relaxor ferroelectrics: Characteristic hierarchical domain configurations and quantitative performances," *Appl. Mater. Today*, vol. 21, p. 100789, Dec. 2020.

[207] K. Fang, W. Jing, and F. Fang, "Multi-scale domain structure observation and piezoelectric responses for [001]-oriented PMN-33PT single crystal," *J. Am. Ceram. Soc.*, vol. 102, no. 12, pp. 7710-7719, Dec. 2019.

[208] L. Li et al., "Machine learning–enabled identification of material phase transitions based on experimental data: Exploring collective dynamics in ferroelectric relaxors," *Sci. Adv.*, vol. 4, no. 3, p. eaap8672, Mar. 2018.

[209] T. Deng, B. Fang, R. Zhu, J. Chen, and H. Luo, "Dynamic scaling hysteresis behavior and field-induced domain transition of 0.16PIN-0.62PMN-0.22PT single crystals," *Curr. Appl. Phys.*, vol. 21, pp. 64-71, Jan. 2021.

[210] Y. Zhang, B. Long, Y. Wen, Z. Zhang, and W. Cao, "Electric field and frequency dependent scaling behavior of dynamic hysteresis in relaxor-based ferroelectric $0.71Pb(Mg_{1/3}Nb_{2/3})O_3$–$0.29PbTiO_3$ single crystal," *J. Alloy. Compd.*, vol. 775, pp. 435-440, Feb. 2019.

[211] T. Jia, Z. Cheng, H. Zhao, and H. Kimura, "Domain switching in single-phase multiferroics," *Appl. Phys. Rev.*, vol. 5, no. 2, p. 021102, Jun. 2018.

[212] Y. Jing et al., "A large and anisotropic enhancement of the mechanical quality factor in ternary relaxor-$PbTiO_3$ single crystals," *Appl. Phys. Lett.*, vol. 118, no. 18, p. 182902, May 2021.

[213] Y. Li et al., "Mn doped ternary relaxor single crystal with high shear piezoelectricity and improved stability," *Ceram. Int.*, vol. 44, no. 15, pp. 18672-18677, Oct. 2018.

[214] S. Zhang, F. Li, J. Luo, R. Xia, W. Hackenberger, and T. R. Shrout, "Investigation of single and multidomain $Pb(In_{0.5}Nb_{0.5})O_3$-$Pb(Mg_{1/3}Nb_{2/3})O_3$-$PbTiO_3$ crystals with mm2 symmetry," *Appl. Phys. Lett.*, vol. 97, no. 13, p. 132903, Sep. 2010.

[215] N. Luo et al., "Crystallographic dependence of internal bias in domain engineered Mn-doped relaxor-$PbTiO_3$ single crystals," *J. Mater. Chem. C*, vol. 4, no. 20, pp. 4568-4576, Apr. 2016.

[216] A. J. Moulson and J. M. Herbert, Electroceramics: materials, properties, applications. John Wiley & Sons, 2003.

[217] Y. Xu, Ferroelectric materials and their applications. Elsevier, 2013.

[218] L. Yang et al., "Evaluation of reversible and irreversible domain wall motions in relaxor ferroelectrics: Influence of acceptor ions," *Appl. Phys. Lett.*, vol. 114, no. 23, p. 232901, Jun. 2019.

[219] R. Wang et al., "Local twin domains and tip-voltage-induced domain switching of monoclinic M_C phase in $Pb(Mg_{1/3}Nb_{2/3})O_3$–$0.34PbTiO_3$ single crystal revealed by piezoresponse force microscopy," *Phys. Rev. B*, vol. 94, no. 5, p. 054115, Aug. 2016.

[220] L. Zheng et al., "Origin of Improvement in Mechanical Quality Factor in Acceptor-Doped Relaxor-Based Ferroelectric Single Crystals," *Phys. Rev. Appl.*, vol. 9, no. 6, p. 064028, Jun 2018.

[221] P. S. Bednyakov, T. Sluka, A. K. Tagantsev, D. Damjanovic, and N. Setter, "Formation of charged ferroelectric domain walls with controlled periodicity," *Sci. Rep.*, vol. 5, no. 1, p. 15819, Oct. 2015.

[222] P. S. Bednyakov, B. I. Sturman, T. Sluka, A. K. Tagantsev, and P. V. Yudin, "Physics and applications of charged domain walls," *npj Comput. Mater.*, vol. 4, no. 1, p. 65, Nov. 2018.

[223] T. Sluka, A. K. Tagantsev, P. Bednyakov, and N. Setter, "Free-electron gas at charged domain walls in insulating $BaTiO_3$," *Nat. Commun.*, vol. 4, no. 1, p. 1808, May 2013.

[224] V. V. Shvartsman, B. Dkhil, and A. L. Kholkin, "Mesoscale Domains and Nature of the Relaxor State by Piezoresponse Force Microscopy," *Annu. Rev. Mater. Res.*, Vol 43, vol. 43, pp. 423-449, Jul. 2013.

[225] V. V. Shvartsman and A. L. Kholkin, "Evolution of nanodomains in $0.9PbMg_{1/3}Nb_{2/3}O_3$-$0.1PbTiO_3$ single crystals," *J. Appl. Phys.*, vol. 101, no. 6, p. 064108, Mar. 2007.

[226] W. He, Q. Li, Y. Sun, X. Xi, Y. Zhang, and Q. Yan, "Investigation of piezoelectric property and nanodomain structures for PIN–PZ–PMN–PT single crystals as a function of crystallographic orientation and temperature," *J. Mater. Chem. C*, vol. 5, no. 9, pp. 2459-2465, Feb. 2017.

[227] W. He, Q. Li, X. Xi, and Q. Yan, "High temperature-insensitive ferro-/piezoelectric properties and nanodomain structures of $Pb(In_{1/2}Nb_{1/2})O_3$–

$PbZrO_3$–$Pb(Mg_{1/3}Nb_{2/3})O_3$–$PbTiO_3$ relaxor single crystals," *J. Am. Ceram. Soc.*, vol. 101, no. 3, pp. 1236-1244, Mar. 2018.
[228] K. Li, E. Sun, X. Qi, B. Yang, J. Liu, and W. Cao, "Dielectric relaxation and local domain structures of ferroelectric PIMNT and PMNT single crystals," *J. Am. Ceram. Soc.*, vol. 103, no. 3, pp. 1744-1754, Mar. 2020.
[229] X. Qi, K. Li, X. Cheng, H. Zheng, E. Sun, and R. Zhang, "The unexpected diffuse phase transition in relaxor-$PbTiO_3$ ferroelectrics via acceptor modification," *Appl. Phys. Lett.*, vol. 123, no. 11, p. 112902, Sep. 2023.
[230] H. Wan, C. Luo, W.-Y. Chang, Y. Yamashita, and X. Jiang, "Effect of poling temperature on piezoelectric and dielectric properties of $0.7Pb(Mg_{1/3}Nb_{2/3})O_3$-$0.3PbTiO_3$ single crystals under alternating current poling," *Appl. Phys. Lett.*, vol. 114, no. 17, p. 172901, Apr. 2019.
[231] Z. Zhang et al., "The performance enhancement and temperature dependence of piezoelectric properties for $Pb(Mg_{1/3}Nb_{2/3})O_3$-$0.30PbTiO_3$ single crystal by alternating current polarization," *J. Appl. Phys.*, vol. 125, no. 3, p. 034104, Jan. 2019.
[232] H. Wan et al., "The overpoling effect of alternating current poling on rhombohedral $Pb(Mg_{1/3}Nb_{2/3})O_3$-$PbTiO_3$ single crystals," *Appl. Phys. Lett.*, vol. 120, no. 19, p. 192901, May 2022.
[233] S. V. Kalinin and D. A. Bonnell, "Imaging mechanism of piezoresponse force microscopy of ferroelectric surfaces," *Phys. Rev. B*, vol. 65, no. 12, p. 125408, Mar. 2002.
[234] D. Phelan et al., "Phase diagram of the relaxor ferroelectric $(1-x)Pb(Mg_{1/3}Nb_{2/3})O_3+xPbTiO_3$ revisited: A neutron powder diffraction study of the relaxor skin effect," *Phase Transit.*, vol. 88, no. 3, pp. 283-305, Mar. 2015.
[235] F. Li, S. Zhang, Z. Xu, and L.-Q. Chen, "The Contributions of Polar Nanoregions to the Dielectric and Piezoelectric Responses in Domain-Engineered Relaxor-$PbTiO_3$ Crystals," *Adv. Funct. Mater.* vol. 27, no. 18, p. 1700310, Mar. 2017.

Jeong-Woo Sun received his B.S. degree in the Department of Materials Science and Engineering from Ulsan National Institute of Science and Technology (UNIST) in 2021. He is a M.S./Ph.D. combined student at UNIST under the supervision of Dr. Wook Jo focusing on the domain engineering of ferroelectric materials.

He joined North Carolina State University (NCSU) as a research scholar in Sep. 2023 under the supervision of Dr. Jong Eun Ryu. His current focus is advanced X-ray experiments and data analysis techniques for relaxor-$PbTiO_3$ single crystals.

Zhengze Xu received his B.S. degree in Electrical Engineering from the University of Pittsburgh in 2020 and completed his M.S. in Mechanical Engineering from the same university in 2022. He is currently pursuing his Ph.D. in Mechanical and Aerospace Engineering at North Carolina State University (NCSU), beginning in August 2023. His research interests lie in the material properties of Mn-doped PIN-PMN-PT and the optimization of AC and DC poling techniques for enhancing the microstructure of single-crystal piezoelectric materials.

Sang-Goo Lee received the M.S. degree in chemical engineering from Yonsei University, Seoul, South Korea, in 1991, and the Ph.D. degree in chemical engineering from Seoul National University, Seoul, in 1995. He was a Manager with the Process Development Team, Hanwha Corporation, from August 1995 to September 1997. He worked on the control of crystal morphology and size in various reaction systems. Energetic materials, like RDX and Penta Erithritol Tetra Nitrate (PETN) require, in order to obtain the more desirable crystal size distribution (CSD). He founded iBULe Photonics and iBULe Humanscan, in 1999. He is currently a CEO of iBULe Photonics. iBULe Photonics successfully developed the single crystal growing technology based on the Bridgman method and is currently producing PMN-PT, PIN-PMN-PT with [001], [011], and [111] growth directions in sizes up to 4.5'' in diameter.

Wook Jo is a professor at the Department of Materials Science and Engineering, Ulsan National Institute of Science and Technology (UNIST), South Korea. Prior to joining the faculty of UNIST inf 2014, he had served as a group leader for the Processing of Ferroelectrics Lab at the Institute of Materials Science, Technische Universität Darmstadt, Germany, since 2007.

His recent research focuses on the functional properties of ferroelectric materials with a special emphasis on lead-free piezoceramics and relaxor ferroelectrics as well as processing and characterization of room-temperature ferromagnetically coupled with ferroelectrics.

Xiaoning Jiang was born in Anhui, China, in 1968. He received the B.S. degree from Shanghai Jiao Tong University, Shanghai, China, in 1990, the M.S. degree from Tianjin University, Tianjin, China, in 1992, and the Ph.D. degree from Tsinghua University, Beijing, China, in 1997.

He was the Chief Scientist and the Vice President of TRS Technologies, Inc., State College, PA, USA, prior to joining North Carolina State University, Raleigh, NC, USA, in 2009, where he is currently the Dean F. Duncan Distinguished Professor and a University Faculty Scholar. His research interests include smart structures and ultrasound transducers for sensing, imaging, therapy, and drug delivery.

Jong Eun Ryu joined NCSU in 2018. Dr. Ryu was an assistant professor at Indiana University-Purdue University Indianapolis (IUPUI) from 2013 to 2018. Dr. Ryu received his Ph.D. in Mechanical Engineering from the University of California, Los Angeles, in 2009 and received his BS and MS degrees from KAIST, Korea, in 2004 and 2006, respectively. Right after his graduate research, Dr. Ryu completed a two-year postdoctoral training course in plasmonic sensors at UCLA. Before he joined IUPUI, he worked for Intel Corp as a senior R&D engineer on advanced semiconductor lithography technology.

His primary research interest lies in harnessing the power of artificial intelligence to revolutionize the design and optimization of multiphysics and multiscale systems. By seamlessly integrating digital simulations and models, we aim to develop robust solutions that address real-world problems. One of the key aspects of our research is the implementation of digital twins for multiphysics systems, allowing us to create virtual counterparts that mirror the behavior of physical systems, enabling accurate predictions and informed decision-making.